

Electronic Supplementary Information (ESI)

Characterization of polymer properties and identification of additives in commercially available research plastics

Amy A. Cuthbertson,^{a,b} Clarissa Lincoln,^{a,b} Joel Miscall,^{a,b} Lisa M. Stanley,^a Anjani K. Maurya,^{b,c} Arun S. Asundi,^{b,c} Christopher J. Tassone,^{b,c} Nicholas A. Rorrer,^{a,b,*} Gregg T. Beckham^{a,b,*}

^a Renewable Resources and Enabling Sciences Center, National Renewable Energy Laboratory, Golden, CO, 80401 USA

^b BOTTLE Consortium, Golden, CO 80401 USA

^c Stanford Synchrotron Radiation Lightsource, SLAC National Accelerator Laboratory, Menlo Park, CA 94025 USA

* Correspondence: nicholas.rorrer@nrel.gov; gregg.beckham@nrel.gov

ESI for the manuscript, including all referenced figures, tables, and text.

Table of Contents

Section I. Analysis of organic and inorganic additives in polymers

Figure S1. Detection of organic additives in PE-2 via ASE GC-MS.

Table S1. Tentative identification of organic additives in PE-2.

Figure S2. Differences in observed additives by analytical method.

Table S2. Sulfur content in polymer substrates.

Figure S3. Trace elements in polymer substrates.

Section II. Structural and thermal characterization

Figure S4. FTIR comparison of EVA substrates.

Figure S5. FTIR comparison of PE substrates.

Figure S6. FTIR comparison of PET substrates.

Figure S7. FTIR comparison of PP substrates.

Figure S8. FTIR comparison of PVC substrates.

Figure S9. FTIR comparison of PS substrates.

Figure S10. FTIR comparison of ABS substrates.

Figure S11. FTIR comparison of nylon substrates.

Figure S12. FTIR comparison of PMMA substrates.

Figure S13. FTIR comparison of PVOH substrates.

Figure S14. FTIR comparison of EVOH substrates.

Table S3. Thermal stability characteristics for polyolefin substrates.

Table S4. Thermal stability characteristics for halogen polymer substrates.

Table S5. Thermal stability characteristics for condensation substrates.

Table S6. Thermal stability characteristics for copolymer substrates.

Table S7. Thermal stability characteristics for acrylic substrates.

Table S8. Tentative identification of additives and degradation products.

Section III. Molar mass and dispersity characterization

Figure S15. Substrates with bimodal molar mass distributions.

Table S9. Comparison of GPC solvents and detectors.

Section IV. Extent of Crystallinity

Figure S16. First heat DSC curve for PET-3.
Figure S17. First heat DSC curve for PLA-1.
Figure S18. First heat DSC trace of nylon-6.
Figure S19. First heat DSC trace of nylon-6,6.
Figure S20. First heat DSC trace of PP-5.
Figure S21. First heat DSC trace of PP-6.
Figure S22. First heat DSC trace of PP-7.
Figure S23. First cooling cycle DSC trace for PS-5.
Figure S24. First heat DSC trace of PAN-1.
Figure S25. First heat DSC trace of EVA-1, 25% vinyl acetate.
Figure S26. First heat DSC trace of EVA-2, 40% vinyl acetate.
Figure S27. First heat DSC trace of PU-1.
Figure S28. SAXS and WAXS patterns for PE-1.
Figure S29. SAXS and WAXS patterns for PE-2.
Figure S30. SAXS and WAXS patterns for PE-7.
Figure S31. SAXS and WAXS patterns for PE-10.
Figure S32. SAXS and WAXS patterns for PE-11.

Section V. Chemical sourcing and substrate preparation

Table S10. Chemical overview.

Text S1. Cyromilling method.

Section VI. Analytical methods

Text S2. GPC methods.

Text S3. HT-GPC methods.

Table S11. GPC measurement conditions by polymer type.

Text S4. Differential Scanning Calorimetry (DSC) Methods.

Equation S1. Percent crystallinity equation.

Table S12. DSC temperature bounds by polymer class.

Equation S2. Standard deviation equations.

Text S5. TGA-FTIR EGA Analysis.

Text S6. SAXS and WAXS Methods.

Text S7. CHNS Method.

Table S13. Elemental Parameters for CHNS Analysis.

Table S14. Ramping conditions for the ultraWAVE digester.

Text S8. Conditions for the ultraWAVE digester.

Text S9. Gas Chromatography Mass Spectrometry Flame Ionization Detection (GC-MS/FID) methods.

Section I. Analysis of organic additives in polymers using mass spectrometry

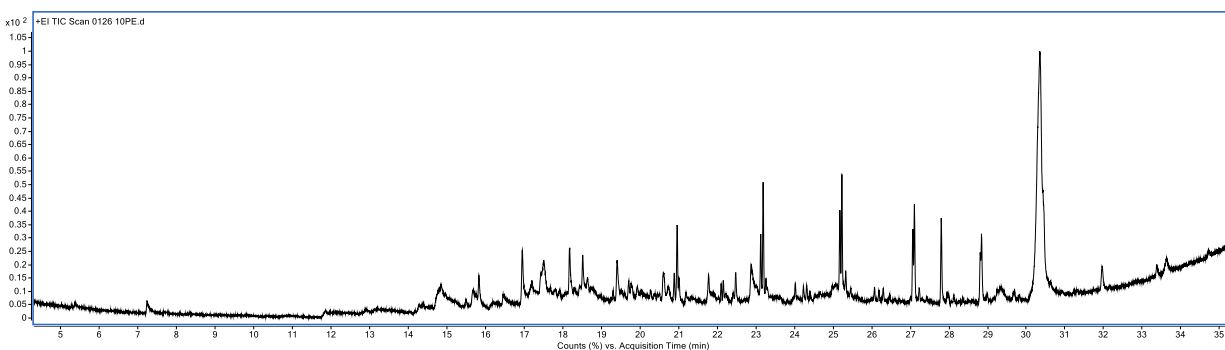


Figure S1. Detection of organic additives in PE-2 via ASE GC-MS. GC-MS chromatogram of PE-2 following ASE extraction with a table of library matches below.

Table S1. Tentative identification of organic additives in PE-2. NIST library matches for PE-2 following ASE extraction and GC-MS.

RT (min)	NIST Library Search	Match %	Comments
17.513	2,4-Di-tert-butylphenol	98	Antioxidant
12.0-18	Mix of paraffins and acids		slip agents
18.637	diethyl phthalate	95	phthalate
19.405	tridecanoic acid	95	fatty acid
30.357	Unknown		

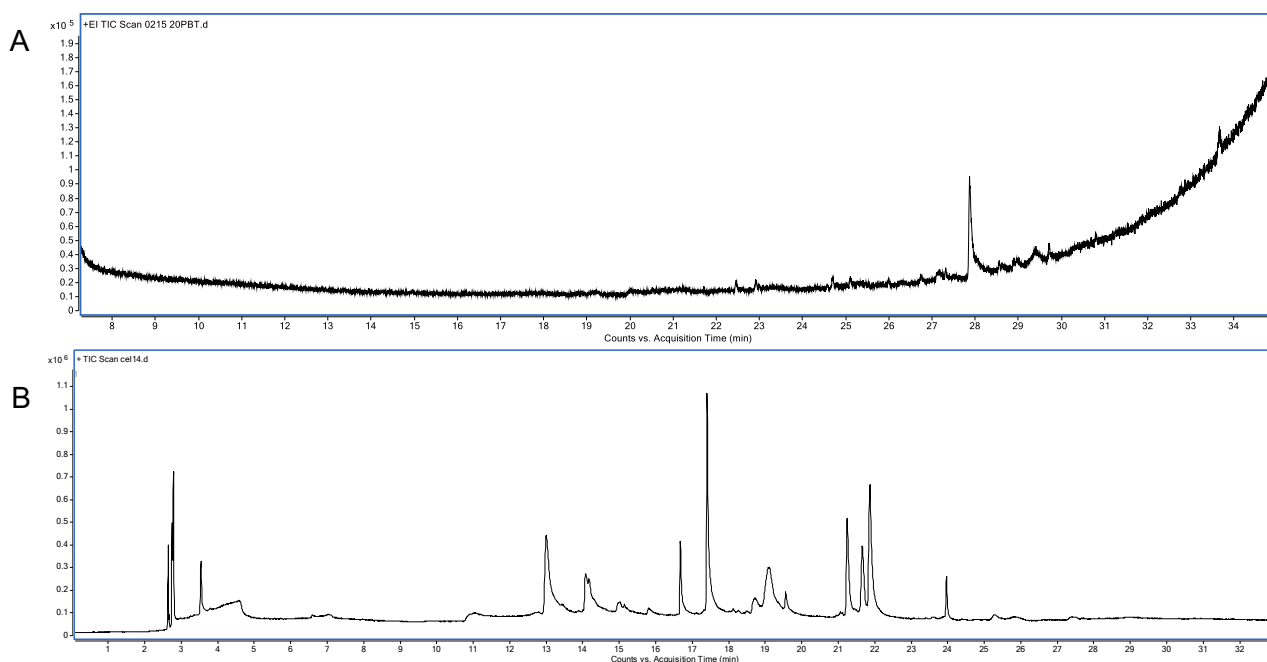


Figure S2. Differences in observed additives by analytical method. (A) GC-MS chromatogram of ASE extracted PBT-1, in which no ASE-extractable additives were observed. (B) PyGC-MS chromatogram of PBT-1, in which many potential additives were observed.

Table S2. Sulfur content in polymer substrates. Summary of substrates containing at least 0.1 wt% sulfur, as determined by S analysis on an elemental determinator.

Substrate Name	Sulfur (wt%)
PMMA-1	0.1
Nylon-66	0.8
EVA-3	0.4
PE-1	0.1
PE-2	0.1
PE-3	0.1
PE-10	0.1
PE-11	0.2
PE-4	0.1
PE-8	0.1
PE-9	0.1
PE-7	0.1

H																	He																														
Li	Be											B	C	N	O	F	Ne																														
Na	Mg											Al	Si	P	S	Cl	Ar																														
K		Sc		V	Cr	Mn	Fe	Co	Ni	Cu	Zn	Ga	Ge	As	Se	Br	Kr																														
Rb	Sr	Y	Zr	Nb	Mo	Tc	Ru	Rh	Pd	Ag	Cd	In	Sn	Sb	Te	I	Xe																														
Cs	Ba		Hf	Ta	W	Re	Os	Ir	Pt	Au	Hg	Tl	Pb	Bi	Po	At	Rn																														
Fr	Ra		Rf	Db	Sg	Bh	Hs	Mt	Ds	Rg	Cn	Uut	Uuq	Uup	Uuh	Uus	Uuo																														
<table border="1"> <tbody> <tr> <td>La</td> <td>Ce</td> <td>Pr</td> <td>Nd</td> <td>Pm</td> <td>Sm</td> <td>Eu</td> <td>Gd</td> <td>Tb</td> <td>Dy</td> <td>Ho</td> <td>Er</td> <td>Tm</td> <td>Yb</td> <td>Lu</td> </tr> <tr> <td>Ac</td> <td>Th</td> <td>Pa</td> <td>U</td> <td>Np</td> <td>Pu</td> <td>Am</td> <td>Cm</td> <td>Bk</td> <td>Cf</td> <td>Es</td> <td>Fm</td> <td>Md</td> <td>No</td> <td>Lr</td> </tr> </tbody> </table>																		La	Ce	Pr	Nd	Pm	Sm	Eu	Gd	Tb	Dy	Ho	Er	Tm	Yb	Lu	Ac	Th	Pa	U	Np	Pu	Am	Cm	Bk	Cf	Es	Fm	Md	No	Lr
La	Ce	Pr	Nd	Pm	Sm	Eu	Gd	Tb	Dy	Ho	Er	Tm	Yb	Lu																																	
Ac	Th	Pa	U	Np	Pu	Am	Cm	Bk	Cf	Es	Fm	Md	No	Lr																																	

Figure S3. Trace elements in polymer substrates. Elements observed at <0.004 wt% levels for any of the studied polymers using ICP-MS.

Section II. Structural and thermal characterization

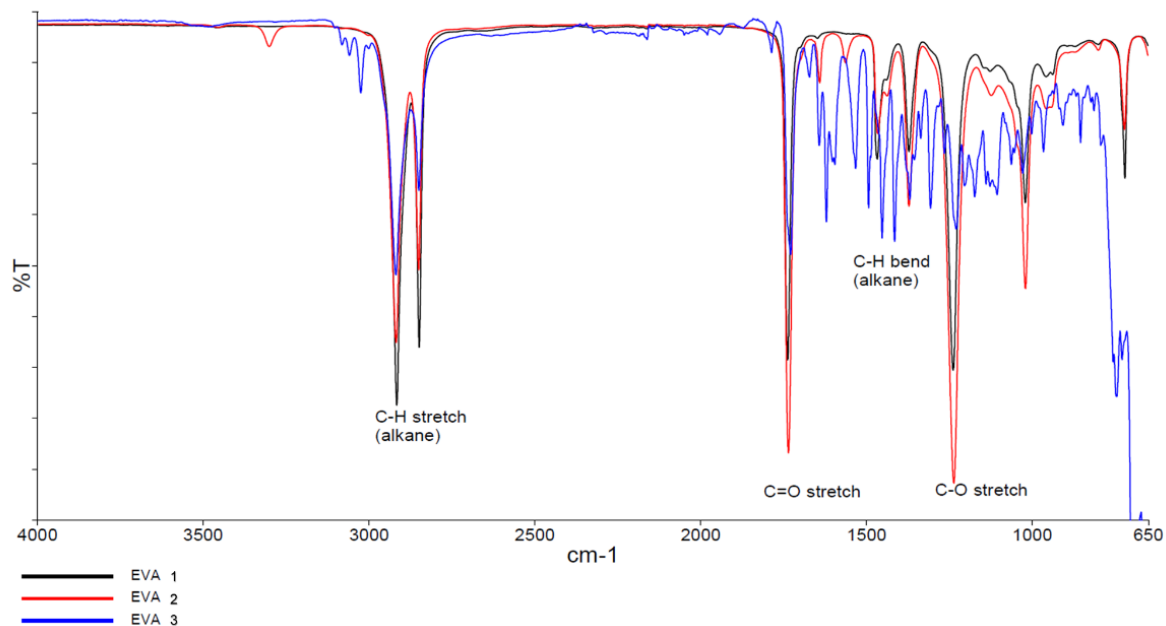


Figure S4. FTIR comparison of EVA substrates. ATR-FTIR spectra overlay of EVA-1, EVA-2, and EVA-3 with labeled functional group peaks. Spectra were scaled to similar intensities.

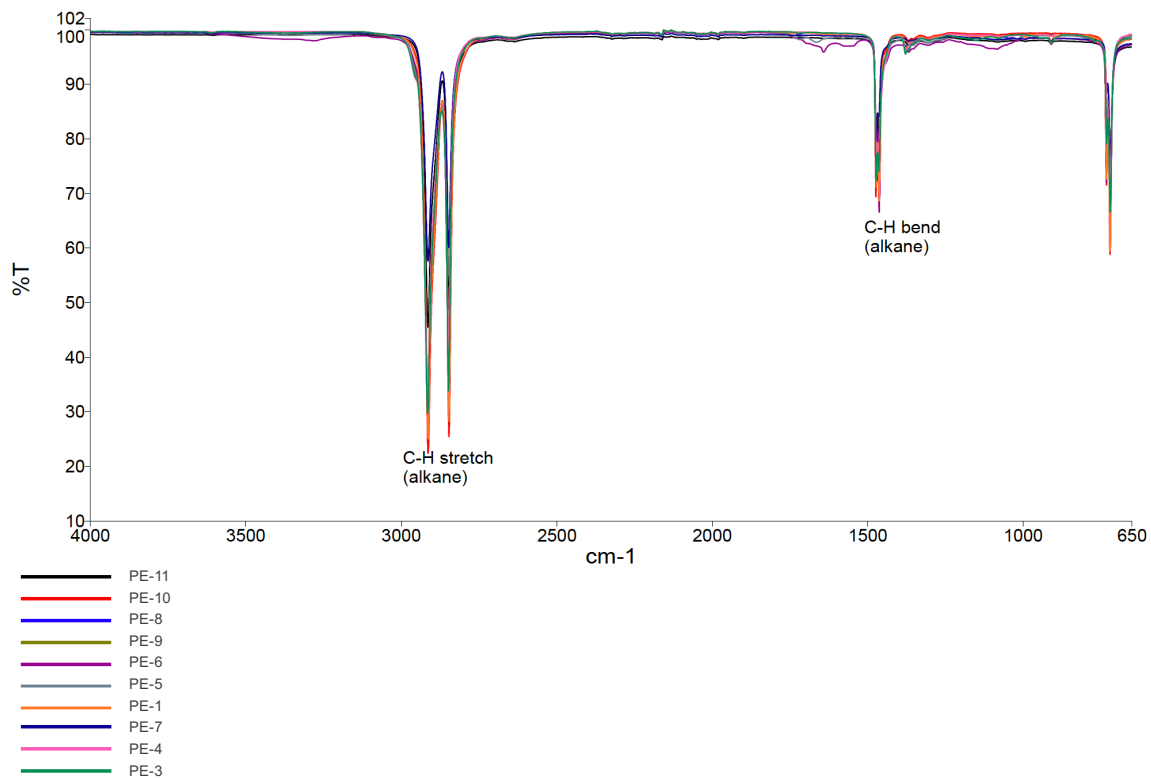


Figure S5. FTIR comparison of PE substrates. ATR-FTIR spectra overlay of PE-1, PE-2, PE-3, PE-4, PE-5, PE-6, PE-7, PE-8, PE-9, PE-10, and PE-11 with labeled functional group peaks. Spectra were scaled to similar intensities.

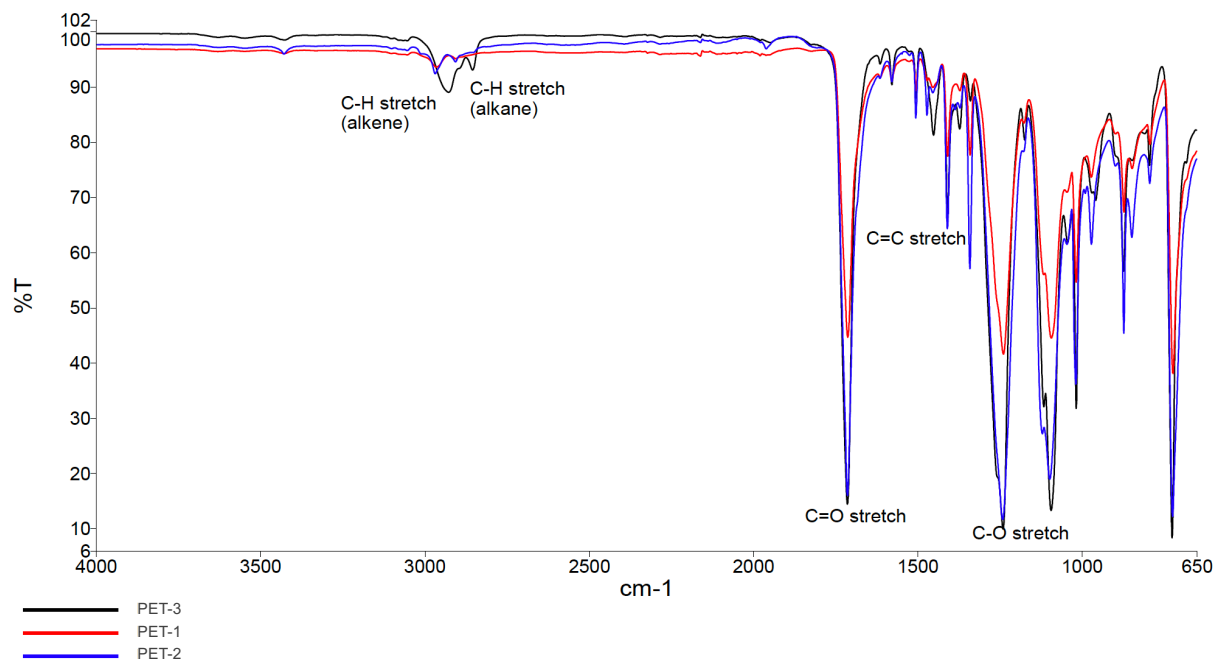


Figure S6. FTIR comparison of PET substrates. ATR-FTIR spectra overlay of PET-1, PET-2, and PET-3 with labeled functional group peaks. Spectra were scaled to similar intensities.

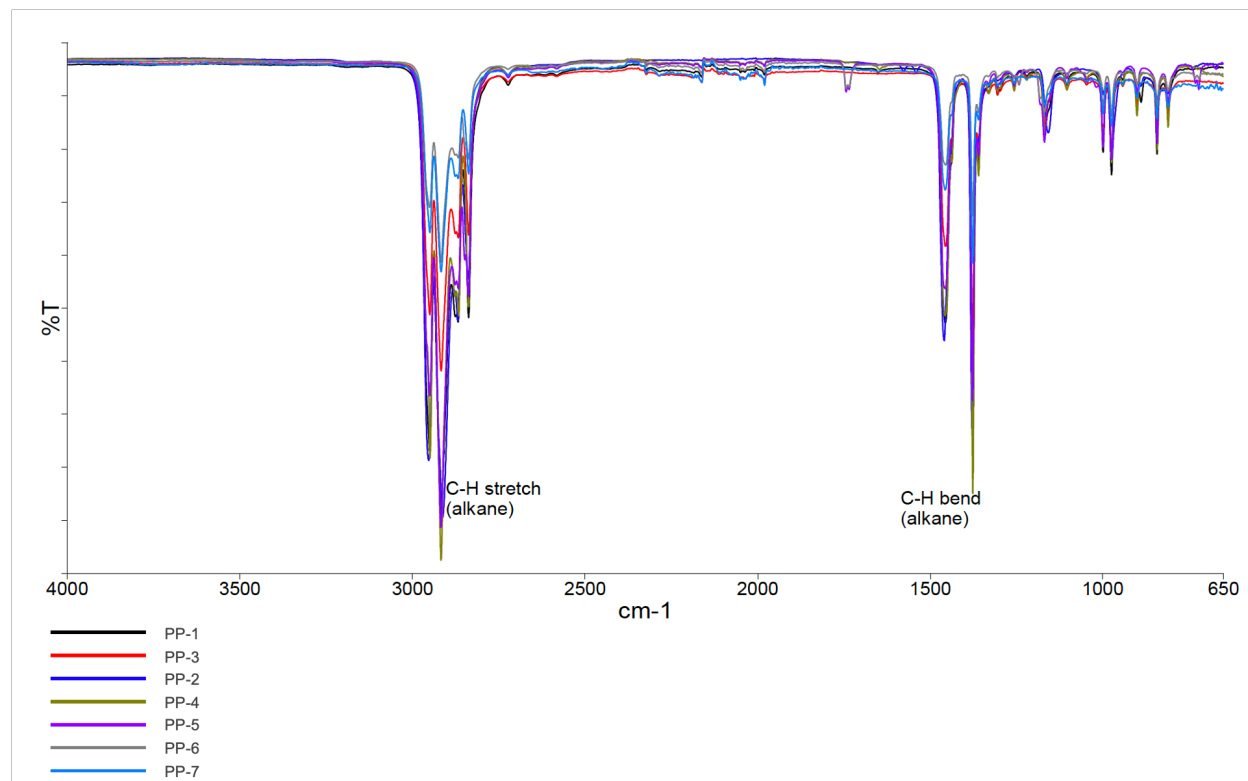


Figure S7. FTIR comparison of PP substrates. ATR-FTIR spectra overlay of PP-1, PP-2, PP-3, PP-4, PP-5, PP-6, and PP-7 with labeled functional group peaks. Spectra were scaled to similar intensities.

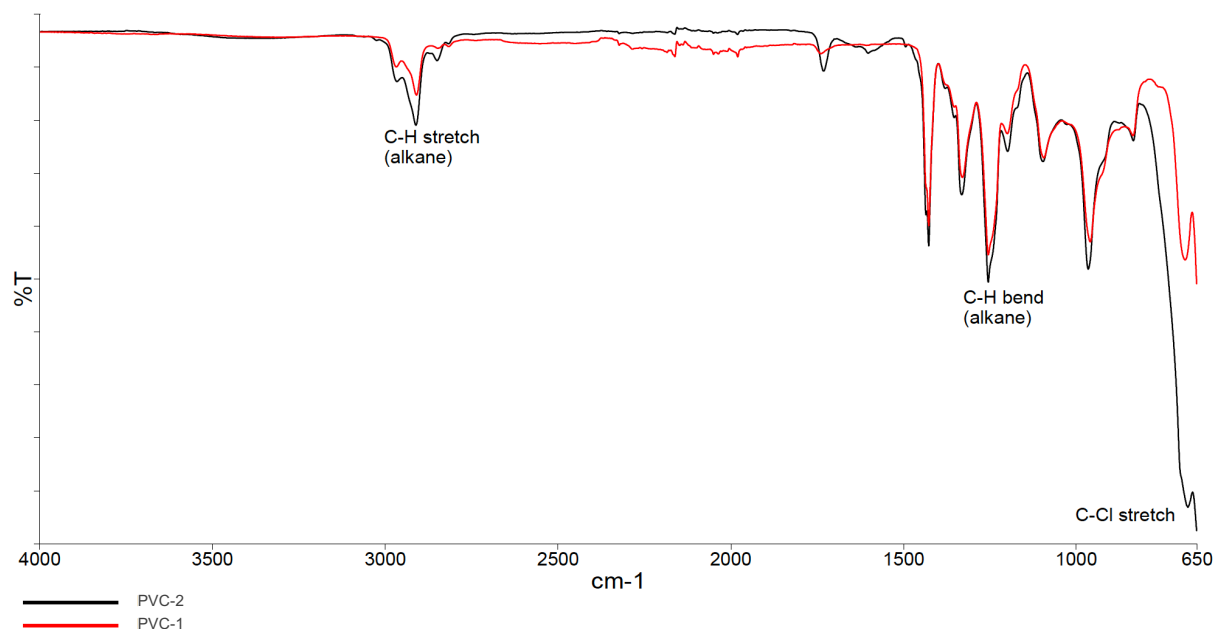


Figure S8. FTIR comparison of PVC substrates. ATR-FTIR spectra of PVC with labeled functional group peaks. Spectra were scaled to similar intensities.

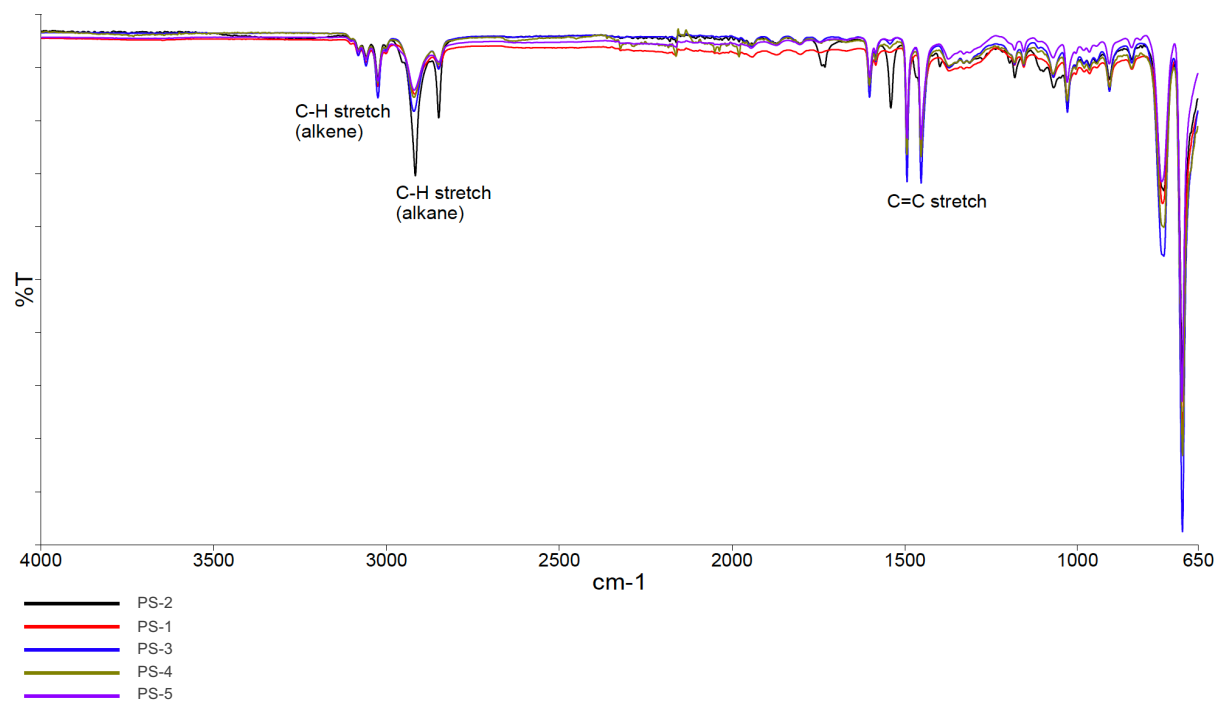


Figure S9. FTIR comparison of PS substrates. ATR-FTIR spectra overlay of PS-1, PS-2, PS-3, PS-4, and PS-5 with labeled functional group peaks. Spectra were scaled to similar intensities.

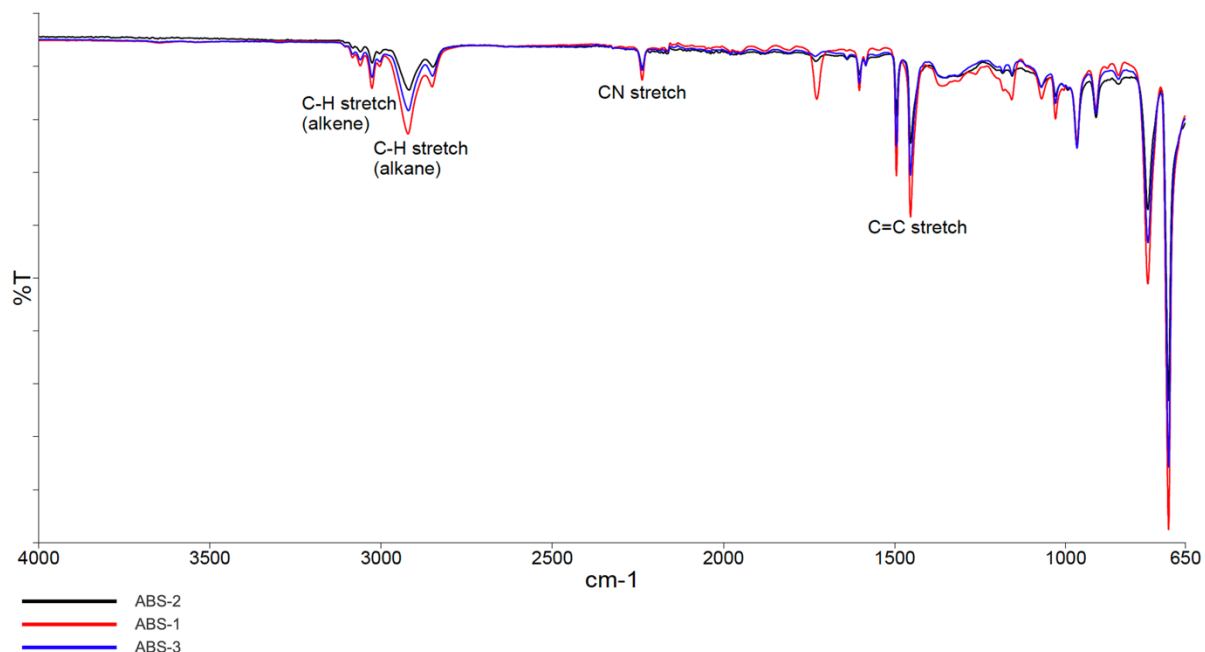


Figure S10. FTIR comparison of ABS substrates. ATR-FTIR spectra overlay of ABS-1, ABS-2, and ABS-3 with labeled functional group peaks. Spectra were scaled to similar intensities.

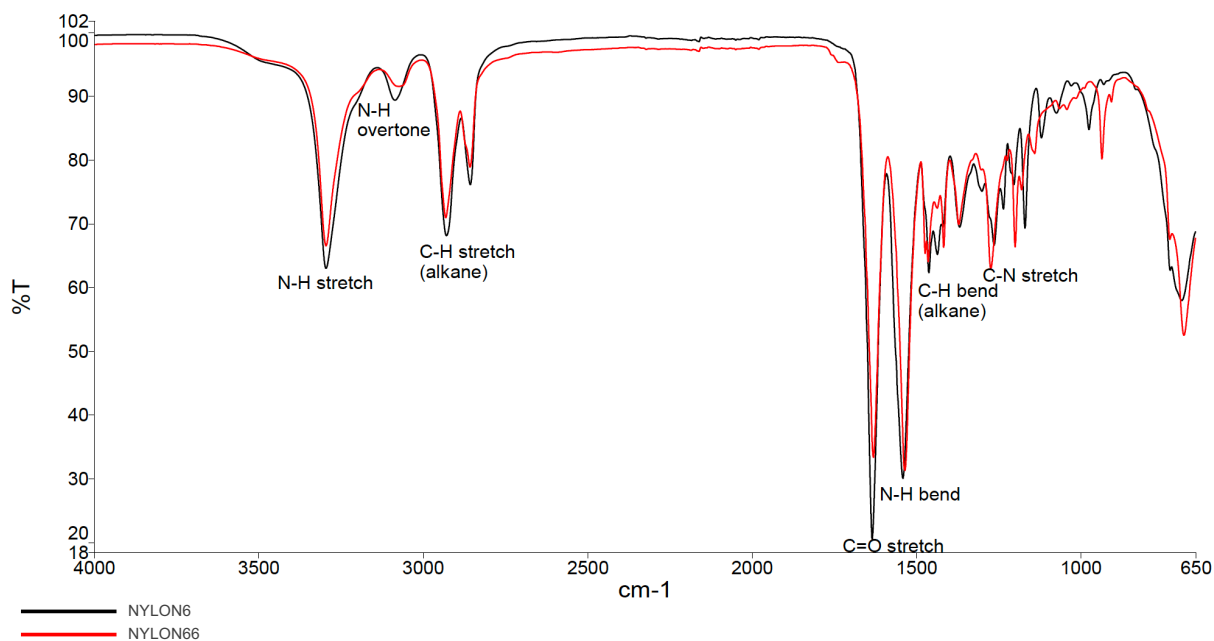


Figure S11. FTIR comparison of nylon substrates. ATR-FTIR spectra overlay of nylon-6 and nylon-6,6 with labeled functional group peaks. Spectra were scaled to similar intensities.

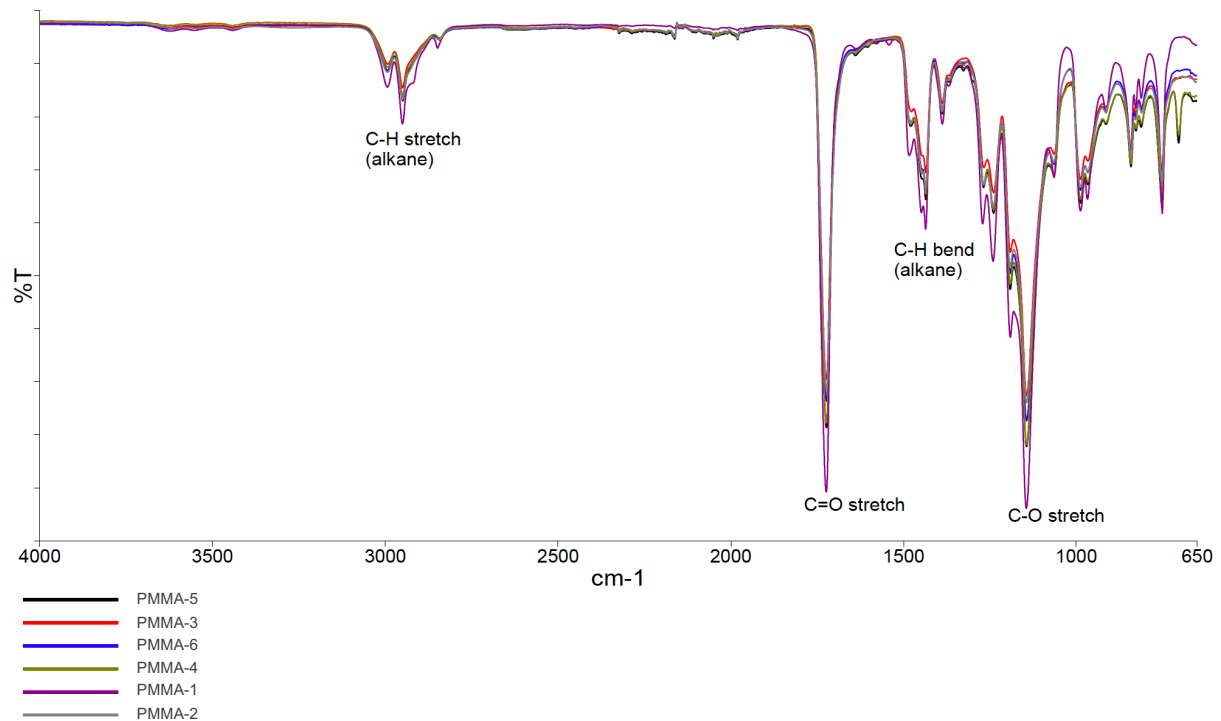


Figure S12. FTIR comparison of PMMA substrates. ATR-FTIR spectra overlay of PMMA-1, PMMA-2, PMMA-3, PMMA-4, PMMA-5, and PMMA-6 with labeled functional group peaks. Spectra were scaled to similar intensities.

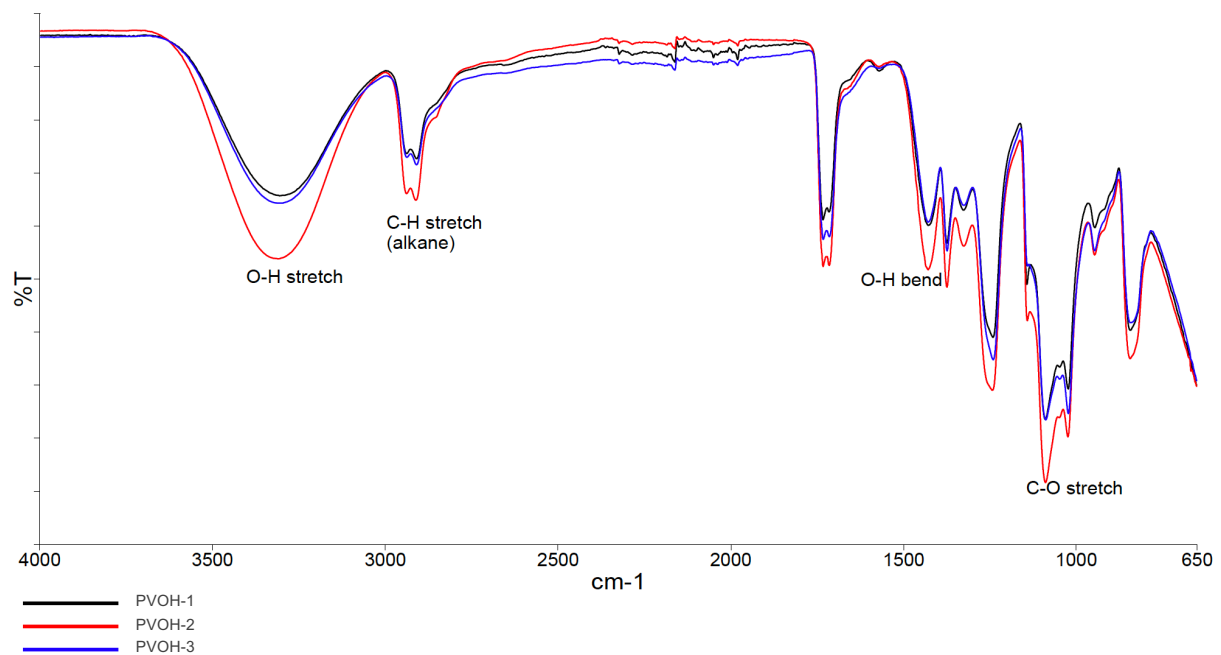


Figure S13. FTIR comparison of PVOH substrates. ATR-FTIR spectra overlay of PVOH-1, PVOH-2, and PVOH-3 with labeled functional group peaks. Spectra were scaled to similar intensities.

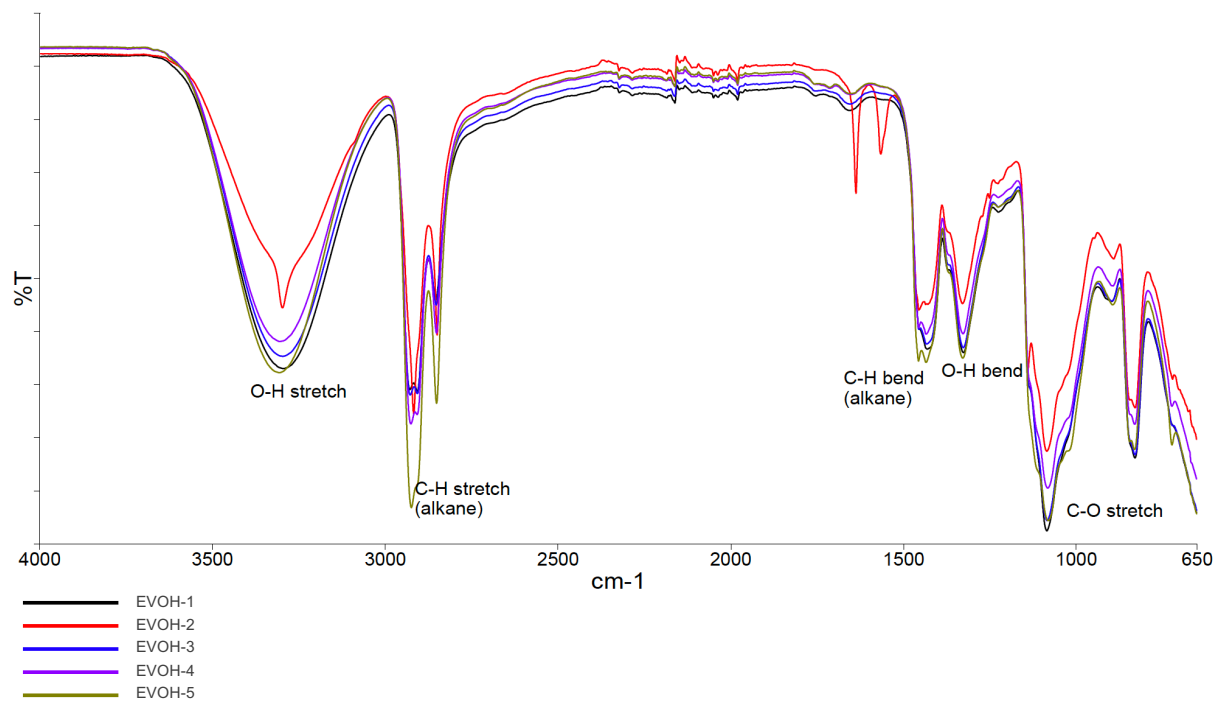


Figure S14. FTIR comparison of EVOH substrates. ATR-FTIR spectra overlay of EVOH-1, EVOH-2, EVOH-3, EVOH-4, and EVOH-5 with labeled functional group peaks. Spectra were scaled to similar intensities.

Table S3. Thermal stability characteristics for polyolefin substrates. TGA results under nitrogen for as received and cryomilled polyolefins including degradation onset temperature, degradation temperature at 50 wt% loss ($T_{d,50}$), residue wt%, and weight loss with derivative max temperatures for each weight loss event. $T_{d,50}$ values are reported only for substrates with only one major weight loss event.

	General			Event 1		Event 2		Event 3	
	Onset (°C)	$T_{d,50}$ (°C)	Residue (wt%)	Mass Loss (weight %)	Derivative Max (°C)	Mass Loss (weight %)	Derivative Max (°C)	Mass Loss (weight %)	Derivative Max (°C)
PE-1 as received	481.4	498.0	0.1	91.3	503.5	-	-	-	-
PE-1 cryomilled	479.9	497.8	0.2	91.8	503.2	-	-	-	-
PE-2 as received	467.9	489.2	0.18	1.6	129.5	87.0	496.7	-	-
PE-2 cryomilled	476.9	495.1	0.2	0.6	130.7	91.5	501.1	-	-
PE-3 as received	452.5	481.8	0.1	89.1	491.1	-	-	-	-
PE-4 as received	460.4	484.5	0.1	92.7	492.0	-	-	-	-
PE-5 as received	464.3	489.4	0.1	93.7	495.1	-	-	-	-
PE-5 cryomilled	466.4	489.5	0.1	92.6	495.8	-	-	-	-
PE-6 as received	483.9	503.0	-0.1	93.1	503.0	-	-	-	-
PE-6 cryomilled	484.5	499.7	-0.3	93.0	504.7	-	-	-	-
PE-7 as received	485.0	501.3	-0.1	92.2	506.2	-	-	-	-
PE-7 cryomilled	482.0	499.9	0.0	90.8	505.8	-	-	-	-
PE-8 as received	468.7	490.0	0.1	93.9	496.1	-	-	-	-
PE-8 cryomilled	471.1	490.0	0.2	92.8	497.5	-	-	-	-
PE-9 as received	467.0	489.9	0.2	92.9	496.8	-	-	-	-
PE-9 cryomilled	467.5	496.5	0.1	93.5	496.5	-	-	-	-
PE-10 as received	487.0	501.9	0.1	93.4	506.7	-	-	-	-
PE-10 cryomilled	484.7	499.8	0.0	92.4	504.2	-	-	-	-
PE-11 as received	485.8	500.3	-0.1	92.9	503.1	-	-	-	-
PE-11 cryomilled	484.3	500.0	0.0	93.2	505.0	-	-	-	-
PP-1 as received	438.2	464.7	0.12	1.3	159.4	86.2	477.4	-	-
PP-1 cryomilled	433.9	462.7	0.1	87.4	475.8	-	-	-	-
PP-2 as received	454.7	475.1	0.0	90.9	482.4	-	-	-	-
PP-2 cryomilled	452.3	474.3	0.2	89.7	481.7	-	-	-	-
PP-3 as received	459.1	477.6	0.1	93.8	483.4	-	-	-	-
PP-3 cryomilled	458.9	476.1	0.1	92.1	481.2	-	-	-	-
PP-4 as received	455.1	475.0	0.2	90.6	481.5	-	-	-	-
PP-4 cryomilled	453.9	474.8	1.8	86.3	481.0	-	-	-	-
PP-7 as received	458.2	476.6	0.2	94.3	482.4	-	-	-	-

PP-7 cryomilled	456.1	476.3	0.2	87.2	481.2	-	-	-	-
PP-6 as received	453.9	476.3	0.1	91.7	481.2	-	-	-	-
PP-6 cryomilled	456.1	474.6	0.0	91.6	480.0	-	-	-	-
PP-5 as received	454.2	475.2	0.3	92.1	480.3	-	-	-	-
PP-5 cryomilled	454.6	479.6	0.3	91.5	479.6	-	-	-	-
PS-1 as received	414.0	434.7	-0.3	94.5	439.9	-	-	-	-
PS-1 cryomilled	411.5	431.7	-0.3	92.9	436.9	-	-	-	-
PS-2 as received	402.4	419.3	1.6	2.3	124.1	0.3	184.1	90.9	422.3
PS-3 as received	414.2	435.3	0.1	94.5	439.9	-	-	-	-
PS-3 cryomilled	412.1	439.0	-0.1	93.8	439.0	-	-	-	-
PS-4 as received	415.2	434.1	-0.2	95.4	439.1	-	-	-	-
PS-4 cryomilled	399.2	432.6	-0.2	92.2	437.8	-	-	-	-
PS-5 as received	408.6	441.1	0.1	81.1	447.7	-	-	-	-
PS-5 cryomilled	414.5	442.0	-0.1	84.3	448.9	-	-	-	-

Table S4. Thermal stability characteristics for halogen polymer substrates. TGA results under nitrogen for as received and cryomilled PVC samples including degradation onset temperature, degradation temperature at 50 wt% loss ($T_{d,50}$), residue wt%, and weight loss with derivative max temperatures for each weight loss event. $T_{d,50}$ values are reported only for substrates with only one major weight loss event.

	General			Event 1		Event 2		Event 3	
	Onset (°C)	$T_{d,50}$ (°C)	Residue (wt%)	Weight Loss (wt%)	Derivative Max (°C)	Weight Loss (wt%)	Derivative Max (°C)	Weight Loss (weight %)	Derivative Max (°C)
PVC-1 as received	279.3	-	7.5	61.6	295.8	27.2	475.8	-	-
PVC-2 as received	297.3	-	19.9	50.3	330.3	23.0	482.7	-	-
PVC-3 cryomilled	292.4	-	19.1	1.0	141.9	59.3	328.5	23.5	471.6

Table S5. Thermal stability characteristics for condensation polymer substrates. TGA results under nitrogen for as received and cryomilled condensation polymers including degradation onset temperature, degradation temperature at 50 wt% loss ($T_{d,50}$), residue wt%, and weight loss with derivative max temperatures for each weight loss event. $T_{d,50}$ values are reported only for substrates with only one major weight loss event.

	General			Event 1		Event 2		Event 3		Event 4	
	Onset (°C)	$T_{d,50}$ (°C)	Residue (wt%)	Weight Loss (wt%)	Derivative Max (°C)	Weight Loss (wt%)	Derivative Max (°C)	Weight Loss (wt%)	Derivative Max (°C)	Weight Loss (wt%)	Derivative Max (°C)
PET-1 as received	430.7	458.4	8.9	84.8	462.1	-	-	-	-	-	-
PET-2 as received	429.2	455.5	9.6	81.9	458.4	-	-	-	-	-	-
PET-2 cryomilled	431.6	456.3	9.6	81.8	456.3	-	-	-	-	-	-
PET-3 as received	432.5	457.7	10.5	78.3	457.4	-	-	-	-	-	-
PET-3 cryomilled	430.5	455.8	10.6	78.8	455.9	-	-	-	-	-	-
PC-1 as received	416.8	505.6	20.4 ¹	72.7	514.3	-	-	-	-	-	-
PC-1 cryomilled	492.6	528.1	19.6 ¹	71.5	527.9	-	-	-	-	-	-
Nylon-6 as received	437.0	466.9	0.05	2.8	129.6	91.0	475.5	-	-	-	-
Nylon-6 cryomilled	438.6	469.2	-0.1	2.2	-	91.8	478.5	-	-	-	-
Nylon-66 as received	428.7	459.2	0.9	2.3	131.1	92.8	465.6	-	-	-	-
Nylon-66 cryomilled	435.4	465.6	0.8	1.2	-	93.3	475.7	-	-	-	-
PBT-1 as received	402.2	421.2	5.4	87.2	422.3	-	-	-	-	-	-
PBT-1 cryomilled	399.5	420.4	5.6	85.1	422.9	-	-	-	-	-	-
PU-1 as received	301.5	-	-0.1	61.6	349.8	35.8	426.5	-	-	-	-
PLA-1 as received	351.4	374.7	0.6	95.5	379.1	-	-	-	-	-	-
PLA-1 cryomilled	351.1	372.1	0.1	94.6	376.2	-	-	-	-	-	-
PHB-1 as received	287.4	-	0.7	4.0	-	75.7	307.5	4.0	353.1	7.2	418.7
PHB-1 cryomilled	285.8	-	0.7	5.5	194.6	75.4	308.1	3.8	352.0	7.3	419.3

¹Weight still decreasing at 800 °C.

Table S6. Thermal stability characteristics for copolymer substrates. TGA results under nitrogen for as received and cryomilled copolymers including degradation onset temperature, degradation temperature at 50 wt% loss ($T_{d,50}$), residue wt%, and weight loss with derivative max temperatures for each weight loss event. $T_{d,50}$ values are reported only for substrates with only one major weight loss event.

	General			Event 1		Event 2		Event 3		Event 4	
	Onset (°C)	$T_{d,50}$ (°C)	Residue (wt%)	Weight Loss (wt%)	Derivative Max (°C)	Weight Loss (wt%)	Derivative Max (°C)	Weight Loss (wt%)	Derivative Max (°C)	Weight Loss (wt%)	Derivative Max (°C)
ABS-1 as received	421.7	443.9	0.9	89.8	444.7	-	-	-	-	-	-
ABS-1 cryomilled	420.9	442.6	0.8	89.5	443.3	-	-	-	-	-	-
ABS-2 as received	424.3	447.7	1.5	89.3	447.0	-	-	-	-	-	-
ABS-2 cryomilled	425.7	448.3	1.4	88.4	449.3	-	-	-	-	-	-
ABS-3 as received	415.0	440.7	0.3	94.5	439.7	-	-	-	-	-	-
ABS-3 cryomilled	420.2	443.7	0.3	94.0	444.0	-	-	-	-	-	-
SAN-1 as received	362.7	-	0.8	2.7	299.7	93.3	399.8	-	-	-	-
SAN-1 cryomilled	405.0	435.3	0.1	1.0	149.3	90.8	435.3	-	-	-	-
PK-1 as received	402.3	429.4	19.2	68.0	424.7	-	-	-	-	-	-
PVOH-1 as received	309.9	-	2.1	3.6	113.3	74.7	336.7	13.6	453.5	-	-
PVOH-1 cryomilled	304.3	-	1.6	3.5	-	76.6	326.8	9.2	453.5	-	-
PVOH-2 as received	310.3	-	2.7	3.2	113.1	64.9	351.7	24.9	451.1	-	-
PVOH-2 cryomilled	300.9	-	1.7	3.7	-	76.2	332.9	11.6	454.1	-	-
PVOH-3 as received	315.8	-	2.8	3.5	124.7	61.1	368.8	28.7	451.9	-	-
PVOH-3 cryomilled	290.1	-	2.0	2.5	-	46.9	322.6	30.9	373.0	12.0	455.5
EVOH-1 as received ¹	379.8	415.5	0.5	0.6	139.7	97.5	422.0	-	-	-	-
EVOH-1 cryomilled ¹	375.8	414.1	0.3	1.8	-	96.5	418.8	-	-	-	-
EVOH-2 as received	277.6	-	1.0	0.9	146.4	76.2	333.5	19.8	468.5	-	-
EVOH-2 cryomilled	275.7	-	0.4	2.0	-	86.7	391.6	8.6	464.6	-	-
EVOH-3 as received ¹	390.0	418.3	0.3	0.8	152.3	92.2	424.0	-	-	-	-
EVOH-3 cryomilled ¹	388.1	414.2	0.3	1.3	49.8	91.2	419.9	-	-	-	-
EVOH-4 as received ¹	389.0	-	0.2	0.8	152.7	85.7	429.0	5.7	466.5	-	-
EVOH-4 cryomilled ¹	387.7	-	0.4	1.1	71.8	78.8	419.4	8.5	471.2	-	-
EVOH-5 as received ¹	402.5	426.8	0.3	0.9	133.9	92.5	431.5	-	-	-	-
EVOH-5 cryomilled ¹	395.2	424.3	0.4	1.3	-	88.1	431.3	-	-	-	-
PVAc-1 as received	330.8	-	3.2	69.1	350.3	24.0	466.8	-	-	-	-
PVAc-1 cryomilled	330.1	-	3.1	67.9	350.8	24.5	472.6	-	-	-	-

EVA-1 as received	337.6	-	0.0	17.8	365.6	80.7	486.5	-	-	-	-
EVA-1 cryomilled	337.2	-	-0.1	16.9	366.2	81.7	488.5	-	-	-	-
EVA-2 as received	334.6	-	0.0	27.8	365.9	70.2	485.4	-	-	-	-
EVA-2 cryomilled	333.3	-	0.3	27.8	366.5	70.0	487.4	-	-	-	-
EVA-3 as received	439.7	466.4	17.8	66.5	465.7	-	-	-	-	-	-
EVA-3 cryomilled	433.5	465.7	17.8	65.6	465.7	-	-	-	-	-	-

¹Poor resolution between weight loss events.

Table S7. Thermal stability characteristics for acrylic substrates. TGA results under nitrogen for as received and cryomilled PMMA samples including degradation onset temperature, degradation temperature at 50 wt% loss ($T_{d,50}$), residue wt%, and weight loss with derivative max temperatures for each weight loss event. $T_{d,50}$ values are reported only for substrates with only one major weight loss event.

	General			Event 1		Event 2		Event 3	
	Onset (°C)	$T_{d,50}$ (°C)	Residue (wt%)	Weight Loss (wt%)	Derivative Max (°C)	Weight Loss (wt%)	Derivative Max (°C)	Weight Loss (wt%)	Derivative Max (°C)
PMMA-1 as received ¹	356.0	-	-0.5	1.4	-	1.6	251.5	87.1	396.8
PMMA-1 cryomilled ¹	358.0	-	0.1	3.2	173.7	5.1	240.4	78.0	388.3
PMMA-2 as received	405.2	427.0	-0.8	94.6	429.6	-	-	-	-
PMMA-3 as received	360.2	390.2	0.4	93.6	394.7	-	-	-	-
PMMA-3 cryomilled	359.4	390.2	0.4	0.7	179.9	94.6	395.1	-	-
PMMA-4 as received	355.2	386.7	0.4	90.2	397.0	-	-	-	-
PMMA-4 cryomilled	344.2	380.2	0.1	2.3	168.7	88.8	387.2	-	-
PMMA-5 as received	351.9	383.9	0.1	0.9	196.4	90.0	391.0	-	-
PMMA-5 cryomilled	343.4	378.3	0.0	2.6	163.8	90.3	386.9	-	-
PMMA-6 as received	347.4	385.7	0.1	92.2	395.1	-	-	-	-
PMMA-6 cryomilled	347.1	379.8	0.0	1.6	167.7	89.9	387.4	-	-

¹Poor resolution between weight loss events.

Table S8. Tentative identification of additives and degradation products. EGA results for 26 polymers with >1 wt% mass loss events other than the major degradation peak determined using TGA-FTIR. All error bars are given as standard deviation from TGA runs (Table S3-7) and TGA-FTIR runs.

Substrate Name	Weight Loss Onset (°C)	Weight Loss (%)	Library Match	Match %
PVC-1	295.0±0.8	52.2±1.2	hydrogen chloride, tetrabromoethane ^b benzene	93.54
	459.9±2.0	27.0±0.8	1-chlorooctane	86.07
PVC-2	148.8±1.3	1.2±0.1	5-norbornene-2,3-dicarboxylic anhydride	77.80
	306.9±0.04	54.0±1.0	hydrogen chloride and benzene	81.91
	450.9±2.3	25.2±0.7	1-chlorooctane	87.07
PVAc-1	342.2±0.4	65.8±1.7	acetic acid	96.02
	458.3±8.3	23.5±1.4	2-nonene or nonadecanenitrile (hydrocarbon or mixture of hydrocarbons)	76.44 ^a
PVOH-1	317.2±0.3	81.6±0.6	acetic acid, acetaldehyde gas, and crotonaldehyde	95.72
	402.8±0.4	10.2±0.4	3-nonanone (long chain hydrocarbon or mixture)	75.16 ^a
PVOH-2	57.5±0.7	1.7±0.3	acetic acid	91.09
	319.0±1.1	73.8±2.0	acetic acid and acetaldehyde gas	90.77
	420.3±1.1	17.7±1.4	3-tridecanone (long chain hydrocarbon or mixture)	86.63
PVOH-3	57.8±1.5	1.6±0.02	acetic acid, 2-butenal, and 3-thiophanone ^c	94.25
	312.1±0.7	46.0±0.2	acetic acid, acetaldehyde gas, and crotonaldehyde	97.16
	353.0±0.6	26.3±0.2	acetaldehyde gas and polyvinyl alcohol-controlled pyrolyzate	75.41
	419.5±0.8	19.3±1.3	3-tridecanone (long chain hydrocarbon or mixture)	87.05
EVA-1	349.6±1.4	15.5±1.0	acetic acid	95.73
	466.1±2.2	78.1±1.9	nonadecanenitrile (long chain hydrocarbon or mixture)	91.65
EVA-2	346.5±0.3	26.9±1.0	acetic acid	96.28
	462.1±1.7	70.4±0.3	nonadecanenitrile (long chain hydrocarbon or mixture)	91.11
EVA-3	442.6±0.8	76.6±1.3	vinylbenzene; dioctylamine, 3-methyl-1-phenyl-3-pentanol	75.89
EVOH-2	344.3±1.9	75.3±1.0	Acetaldehyde; 14-pentadecene-2,5-dione; 1,2,5-pentanetriol	92.90
	428.9±1.7	15.7±0.6	3-eicosanone (long chain hydrocarbon or mixture)	89.10
EVOH-1	345.3±0.6	81.0±2.7	acetaldehyde; 2,5-dihydroxy-dioctyl ester 1,4-cyclohexadiene-1,4-dicarboxylic acid; 4-hydroxy-3-methyl butanone	93.40
	426.0±4.0	12.3±1.2	3-eicosanone (long chain hydrocarbon or mixture)	89.60
EVOH-3	367.0±3.3	78.8±1.9	acetaldehyde; 2,5-dihydroxy-dioctyl ester 1,4-cyclohexadiene-1,4-dicarboxylic acid; 4-hydroxy-3-methyl butanone	93.4

	436.0±4.0	14.5±1.0	1,12-dihydroxyoctadecane; ethyl 2-acetyl-5-chloropentanoate ^d	90.83
EVOH-4	406.9±1.2	91.4±0.004	acetaldehyde; 2-nonanone; 1,5-pentanediol	88.92
EVOH-5	364.4±5.4	73.3±1.4	acetaldehyde; 2,5-dihydroxy-dioctyl ester 1,4-cyclohexadiene-1,4-dicarboxylic acid; 4-hydroxy-3-methyl butanone	92.58
	442.8±3.1	22.0±0.2	3-eicosanone (long chain hydrocarbon or mixture)	90.96
PMMA-1	185.8±4.7	11.5±1.0	methacrylic acid methyl ester	92.90
	357.4±1.8	85.3±1.1	methacrylic acid methyl ester	95.76
PMMA-3	71.1±0.5	1.0±0.1	methacrylic acid methyl ester	78.21 ^a
	366.2±2.1	97.0±0.4	methacrylic acid methyl ester	95.77
PMMA-4	161.1±4.1	2.6±0.3	methacrylic acid methyl ester	94.29
	354.9±3.6	93.5±1.4	methacrylic acid methyl ester	95.77
PMMA-5	161.6±2.0	2.7±0.2	methacrylic acid methyl ester	96.04
	352.5±0.6	93.2±0.9	methyl methacrylate and 3-phenylpropyl formate	97.05
PMMA-6	176.9±1.5	2.0±0.2	methacrylic acid methyl ester	87.53
	355.3±1.2	95.5±0.2	methacrylic acid methyl ester	96.22
Nylon-6	450.8±1.2	96.0±0.8	hexahydro-2-azepinone	88.97
Nylon-66	423.1±4.4	95.7±1.2	ammonia; N-nitrosodicyclohexylamine; quinoxalinone; 1,5-diamino-2-methylpentane; butyric acid hydrazide	93.73
PS-2	127.4±2.5	1.7±0.1	pentane	97.01
	419.5±1.6	96.7±0.5	styrene and bibenzyl	97.66
PE-2	168.2±0.04	1.0±0.3	butyl hydroxy toluene	65.08 ^a
	475.5±0.6	98.4±0.6	1-eicosene (long chain hydrocarbon or mixture)	92.60
PAN-1	330.5±0.6	44.2±0.4	ammonium sulfamate ^c ; succinonitrile	71.12 ^a
	377.1±2.6	17.6±0.6	ammonia	93.82
PHB-1	190.1±0.2	5.0±0.1	citric acid tripropyl ester and 1-cyclopenten-3-one	76.89
	306.5±1.6	76.4±1.7	adipic acid monomethyl ester	71.44
	337.1±1.2	3.9±0.1	2-butenic acid and glacial acetic acid	89.36
	413.9±1.7	9.6±1.6	2-butenic acid and 2-butenic acid methyl ester	90.03
PU-1	326.8±0.4	48.2±2.7	cyclohexyl isocyanic acid and 1,7-heptanediol	91.67
	429.7±0.8	45.4±0.1	1,2-dibutoxyethane	85.44
SAN-1	407.2±1.0	97.0±0.5	styrene; 3-phenylpropyl mercaptan ^c	91.15

^aNoise in FTIR background likely causes low match percent.

^bNo Br observed in ICP-MS data.

^cNo S observed in CHNS data.

^dNo Cl observed in ICP-MS data.

Section III. Molar mass and dispersity characterization

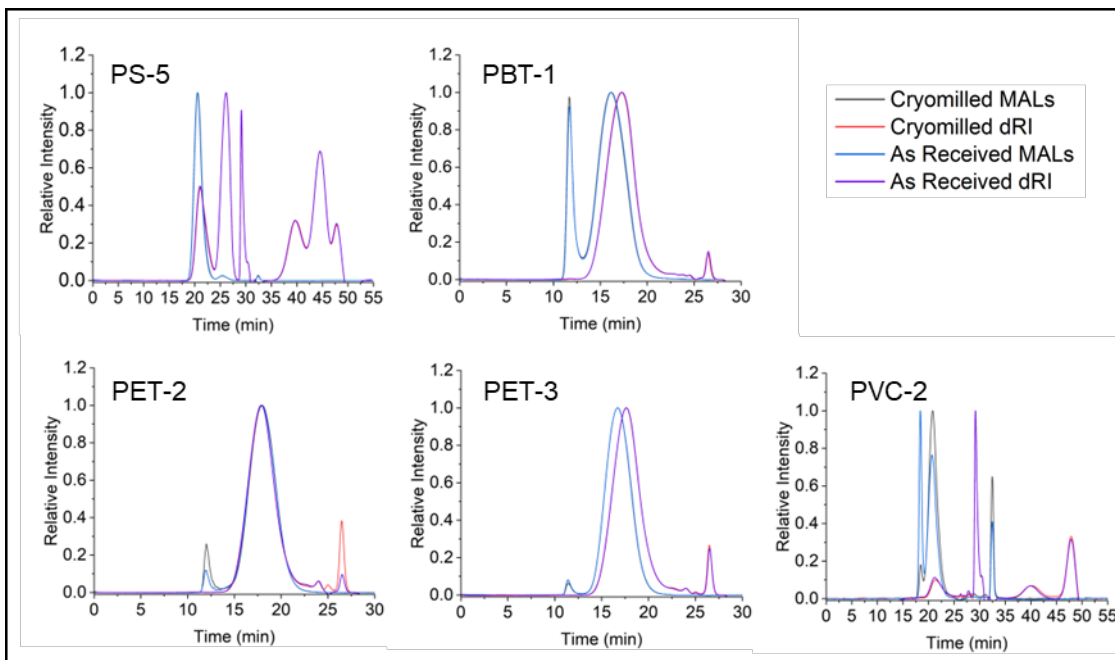


Figure S15. Substrates with bimodal molar mass distributions. GPC traces for as received and cryomilled samples including PS-5, PBT-1, PC-1, PET-2, PET-3, and PVC-2. PS-5 has two molar mass distributions at 21 min and 26 min, PBT-1 at 11 min and 17 min, PET-2 at 12 min and 17 min, PET-3 at 11 min and 17min, and PVC-2 at 18 min and 21 min.

Table S9. Comparison of GPC solvents and detectors. Comparison of the number average molecular mass (Mn), weight average molecular mass (Mw), and dispersity (Đ) of polystyrene substrates using tetrahydrofuran (THF) and trichlorobenzene (TCB).

Substrate Name	Using 100% Mass Recovery				Using Literature dn/dc				Using Column Calibration ²		
	Mn (kDa)	Mw (kDa)	Đ	est. dn/dc	Mn (kDa)	Mw (kDa)	Đ	dn/dc	Mn (kDa)	Mw (kDa)	Đ
PS-1 as received	183.4	411.8	2.2	0.113	115.3	258.9	2.2	0.184	143.4	230.8	1.6
PS-1 cryomilled	155.9	390.6	2.5	0.113	98.3	246.2	2.5	0.184	134.3	222.8	1.7
PS-2 as received	164.9	338.0	2.0	0.111	102.3	209.6	2.0	0.184	129.3	192.8	1.5
PS-3 as received	146.3	405.8	2.8	0.120	97.4	270.3	2.8	0.184	149.0	224.2	1.5
PS-3 cryomilled	145.8	333.8	2.3	0.116	94.3	215.8	2.3	0.184	119.8	181.0	1.5
PS-4 as received	210.1	415.4	2.0	0.114	132.9	262.8	2.0	0.184	142.1	215.9	1.5
PS-4 cryomilled	205.3	406.5	2.0	0.113	129.3	256.1	2.0	0.184	132.7	200.5	1.5
PS-5 as received peak 1	N/A ¹				60.3	113.6	1.9	0.184	88.1	126.2	1.4
PS-5 cryomilled peak 1					55.8	108.4	1.9	0.184	82.5	120.2	1.5
PS-5 as received peak 2					1.34	1.83	1.4	0.184	1.1	1.5	1.3
PS-5 cryomilled peak 2					1.18	1.70	1.4	0.184	0.2	1.5	6.5

¹100% Mass recovery cannot be used with multiple peaks.

²HT-GPC is not equipped with a MALS, so dn/dc is not used.

Section IV. Extent of Crystallinity

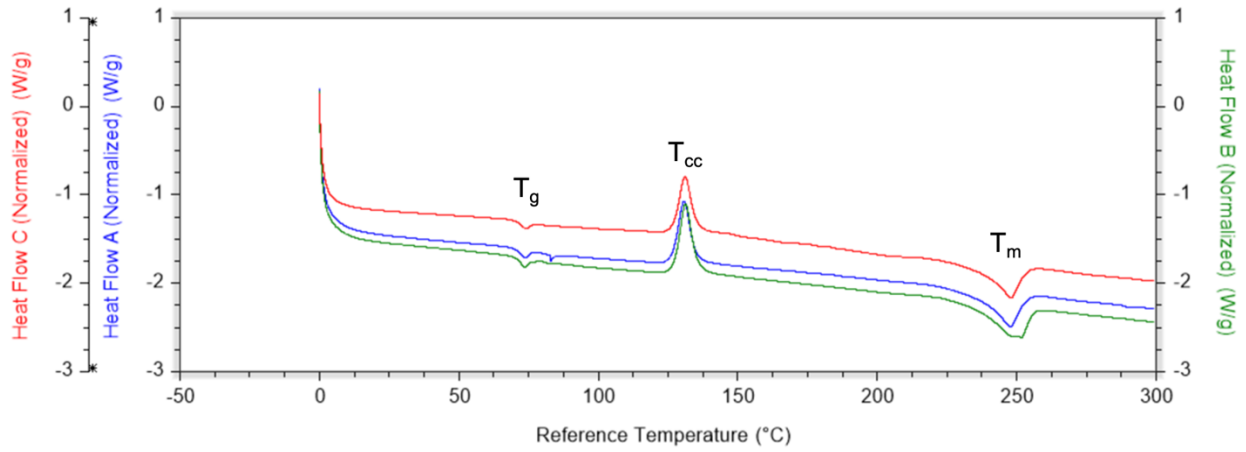


Figure S16. First heat DSC curve for PET-3. DSC trace for the first heating ramp from 0 °C to 300 °C with the glass transition temperature (T_g), the cold crystallization temperature (T_{cc}), and the melting temperature (T_m) well resolved. The three traces (A, B, and C) represent simultaneous triplicate measurements.

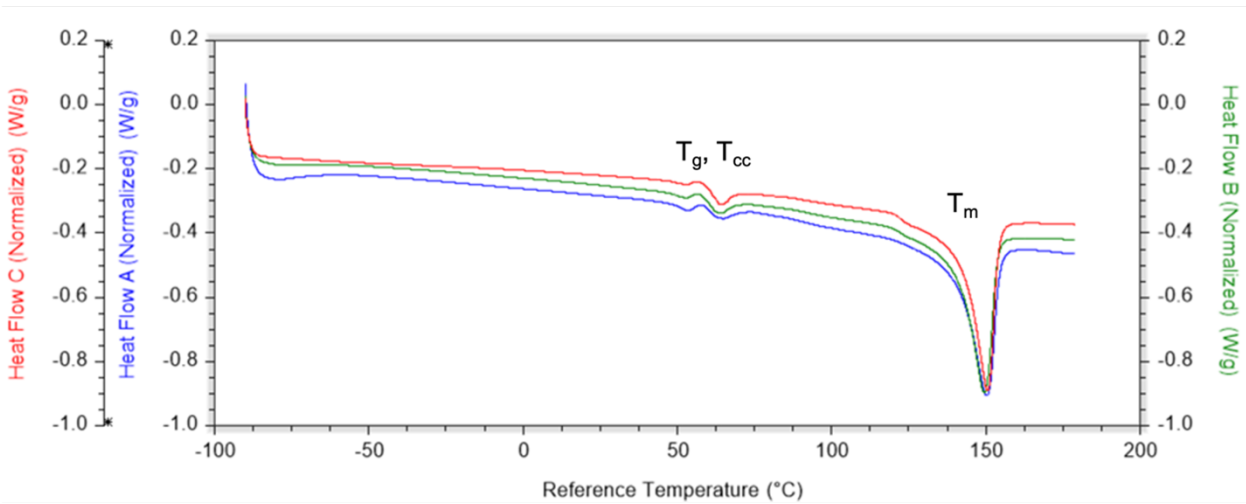


Figure S17. First heat DSC trace for PLA-1. DSC trace for the first heating ramp from -90 °C to 180 °C. T_g and T_{cc} appear to occur simultaneously. The three traces (A, B, and C) represent simultaneous triplicate measurements.

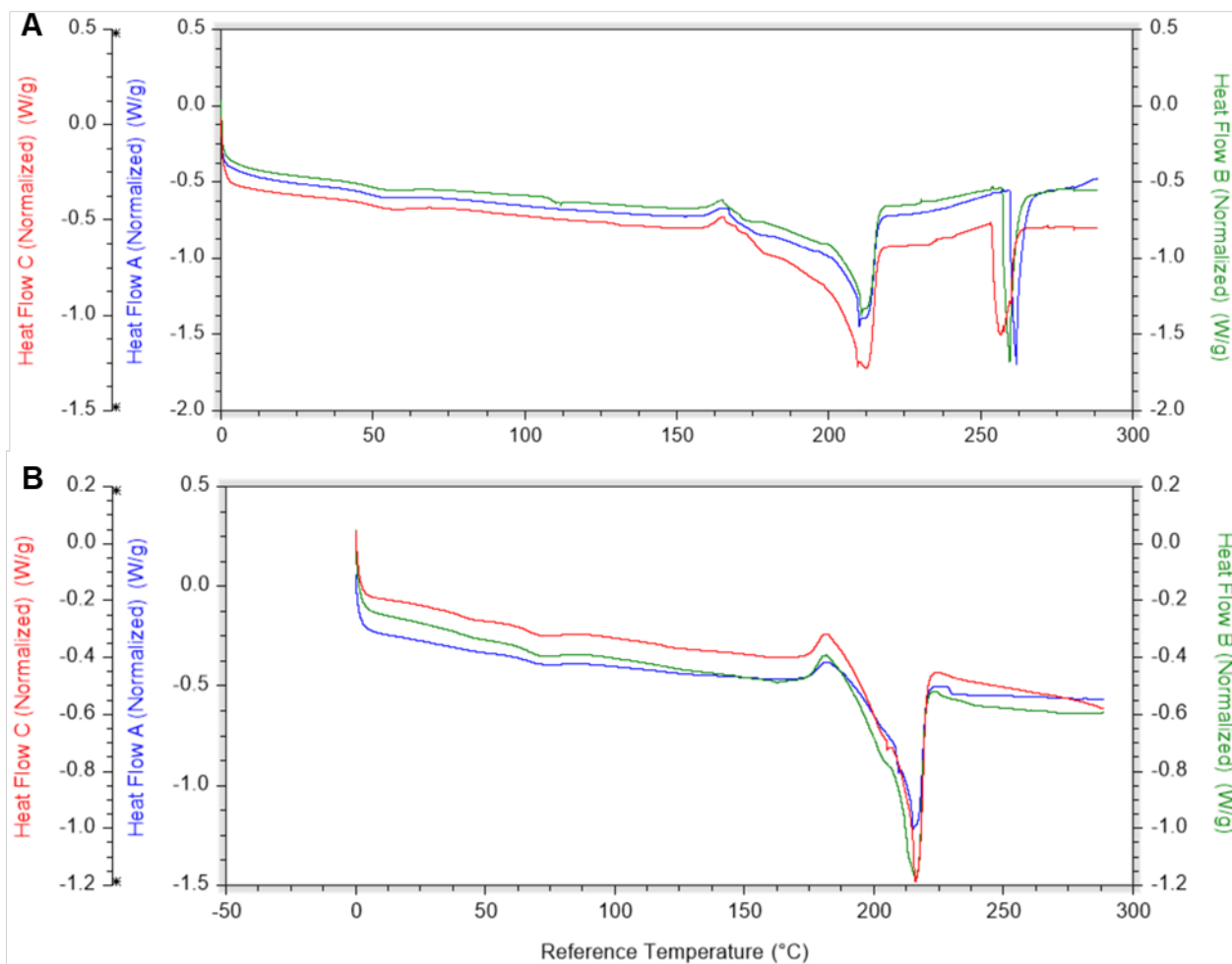


Figure S18. First heat DSC trace of nylon-6. DSC trace for the first heating ramp from 0 °C to 290 °C. The three traces (A, B, and C) represent simultaneous triplicate measurements. Pane (A) is undried nylon-6 and pane (B) is dried nylon-6. Note the disappearance of the endotherm around 260°C after drying, indicating the presence of water.

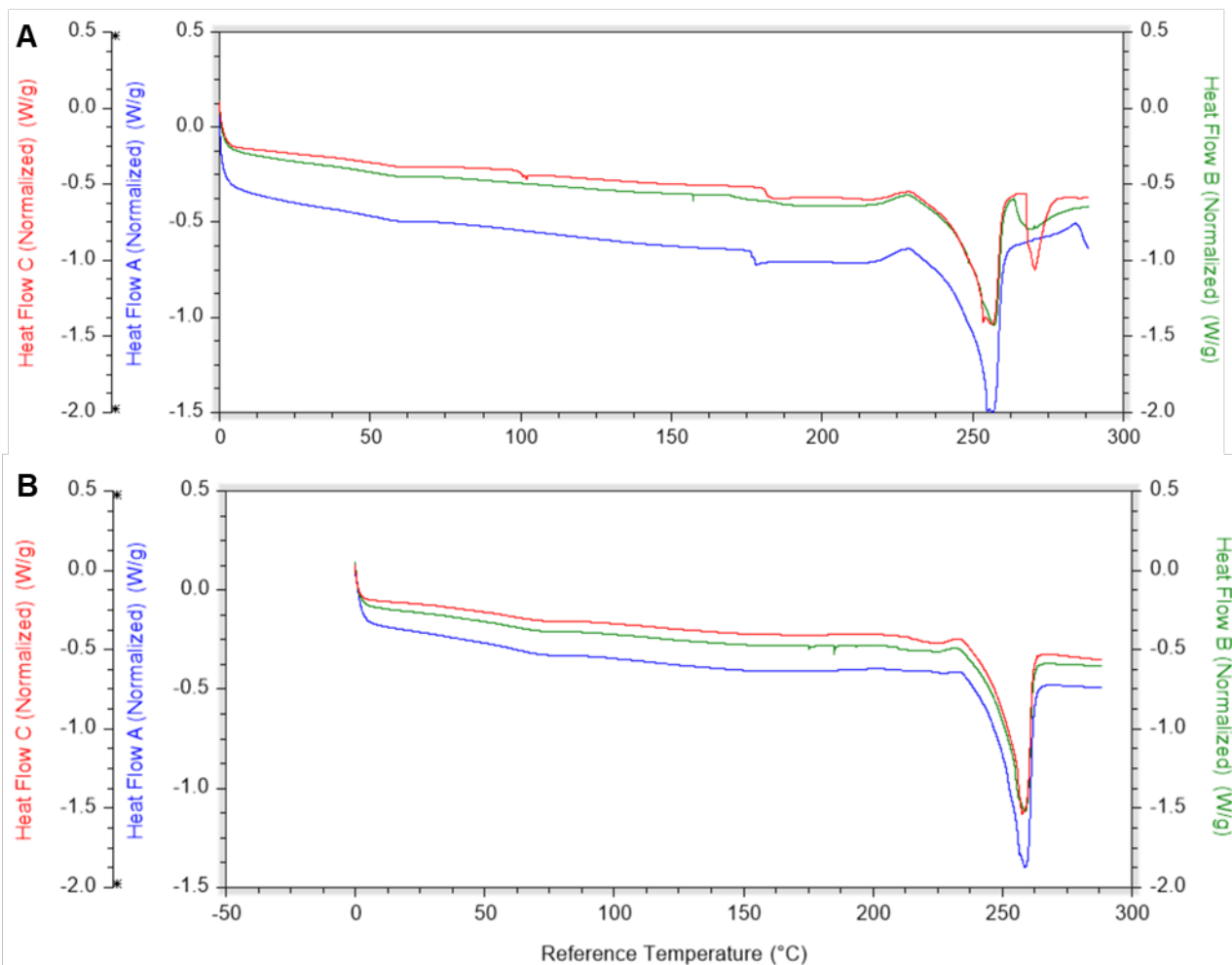


Figure S19. First heat DSC trace of nylon-6,6. DSC trace for the first heating ramp from 0 °C to 290 °C. The three traces (A, B, and C) represent simultaneous triplicate measurements. Pane **(A)** is undried nylon-6,6, and pane **(B)** is dried nylon-6,6. Note the disappearance of the endotherm around 260°C after drying, indicating the presence of water.

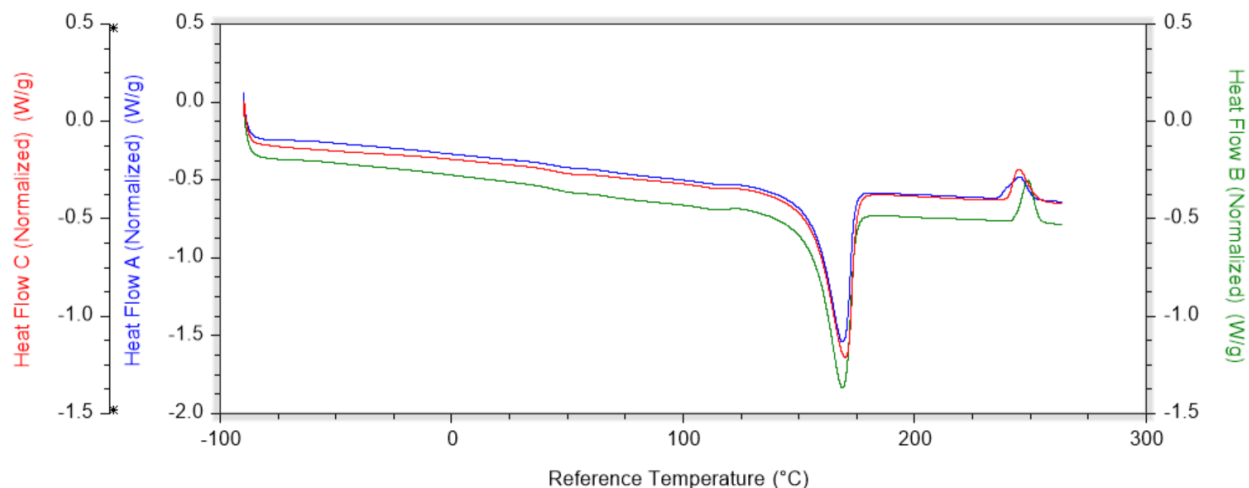


Figure S20. First heat DSC trace for PP-5. DSC trace for the first heating ramp from -90 °C to 265 °C. The three traces (A, B, and C) represent simultaneous triplicate measurements.

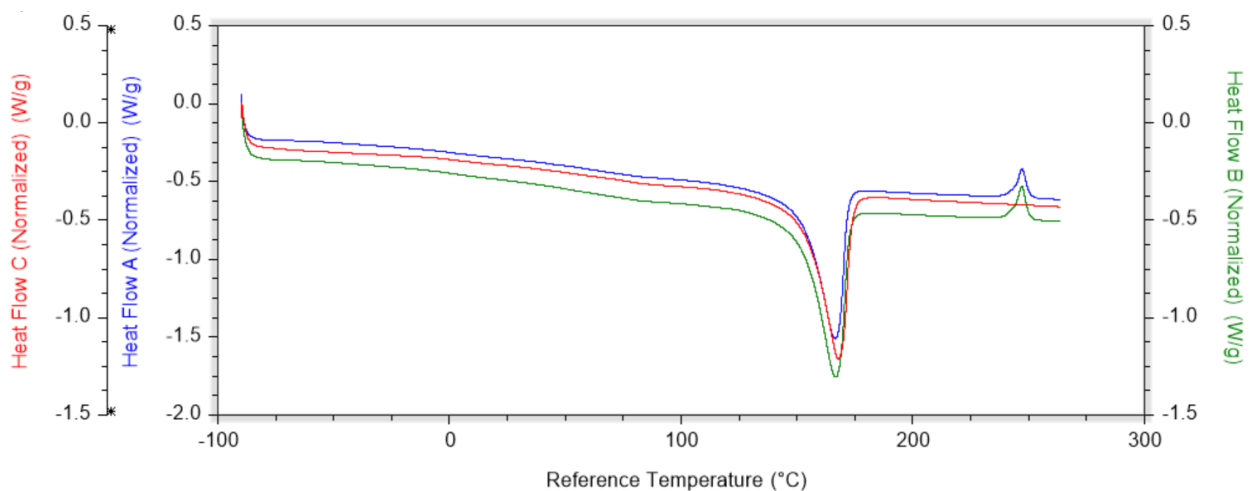


Figure S21. First heat DSC trace for PP-6. DSC trace for the first heating ramp from -90 °C to 265 °C. The three traces (A, B, and C) represent simultaneous triplicate measurements.

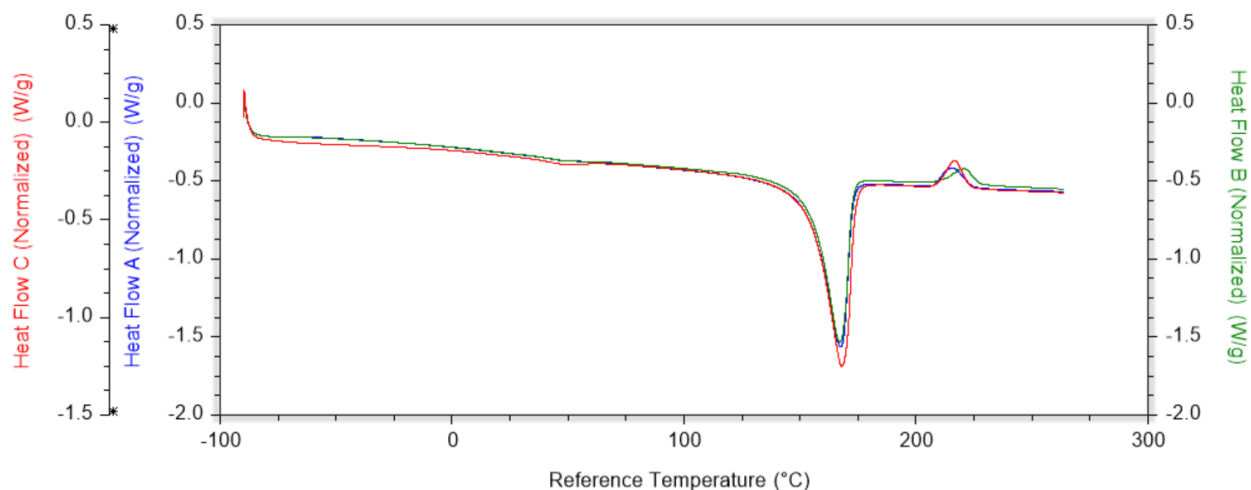


Figure S22. First heat trace for PP-7. DSC trace for the first heating ramp from -90 °C to 265 °C. The three traces (A, B, and C) represent simultaneous triplicate measurements.

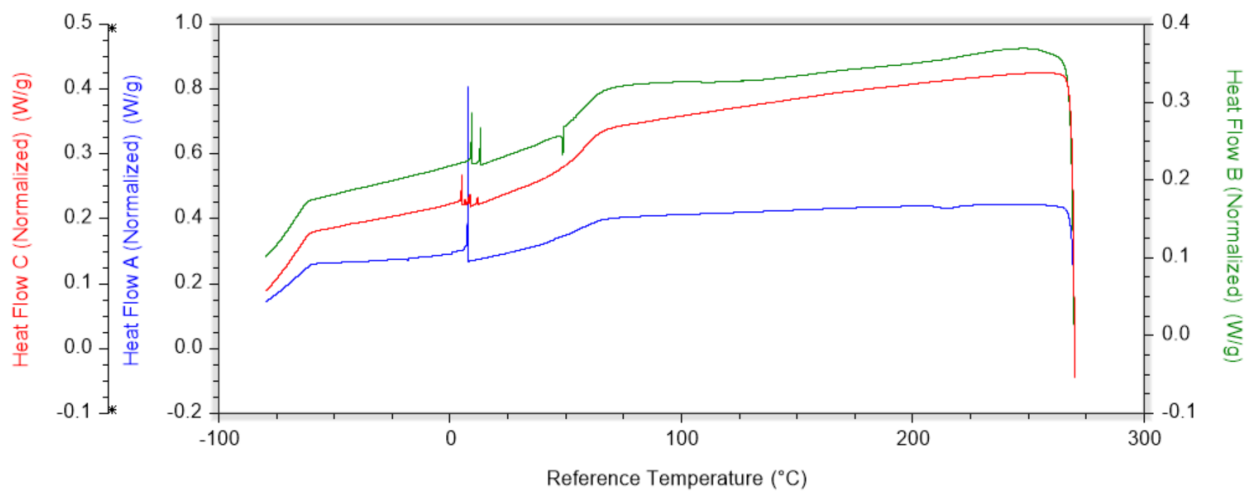


Figure S23. First cooling cycle DSC trace for PS-5. DSC trace for the first cooling ramp from 270 °C to -90 °C. The three traces (A, B, and C) represent simultaneous triplicate measurements.

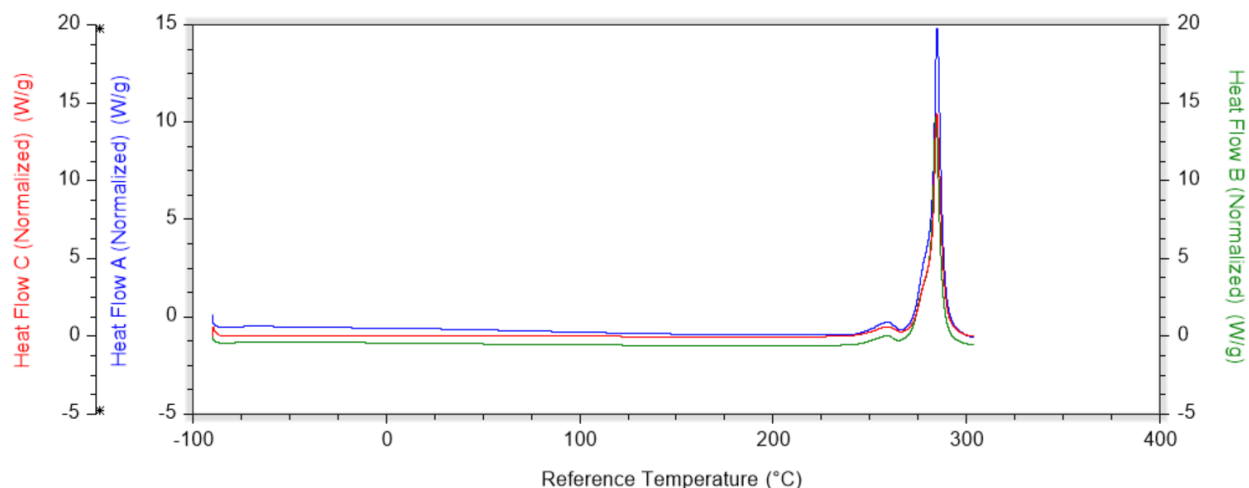


Figure S24. First heat DSC trace of PAN-1. DSC trace for the first heating ramp from -90 °C to 215 °C. The three traces (A, B, and C) represent simultaneous triplicate measurements.

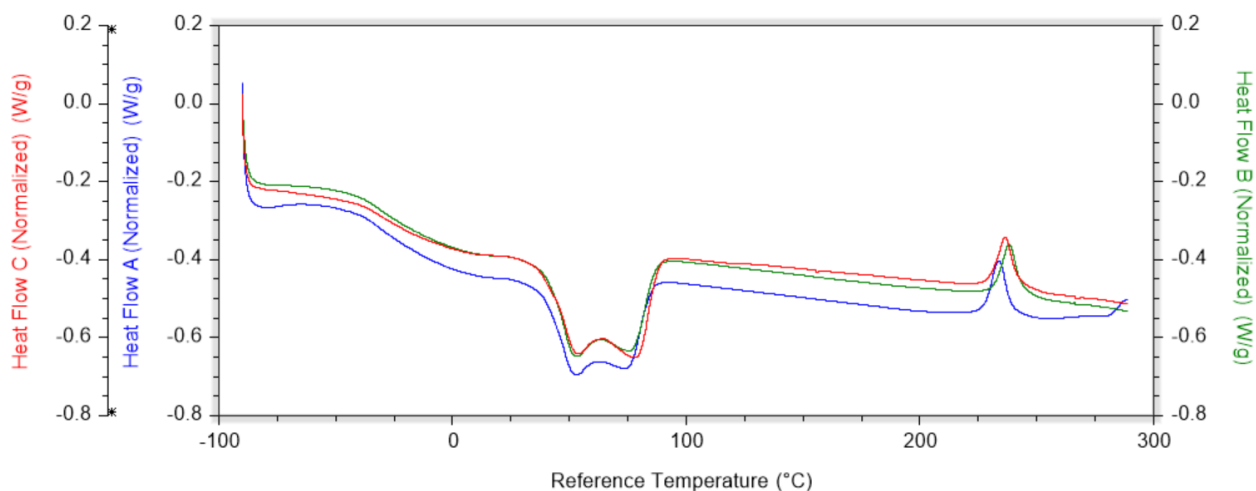


Figure S25. First heat DSC trace of EVA-1, 25% vinyl acetate. DSC trace for the first heating ramp from -90 °C to 290 °C. The three traces (A, B, and C) represent simultaneous triplicate measurements.

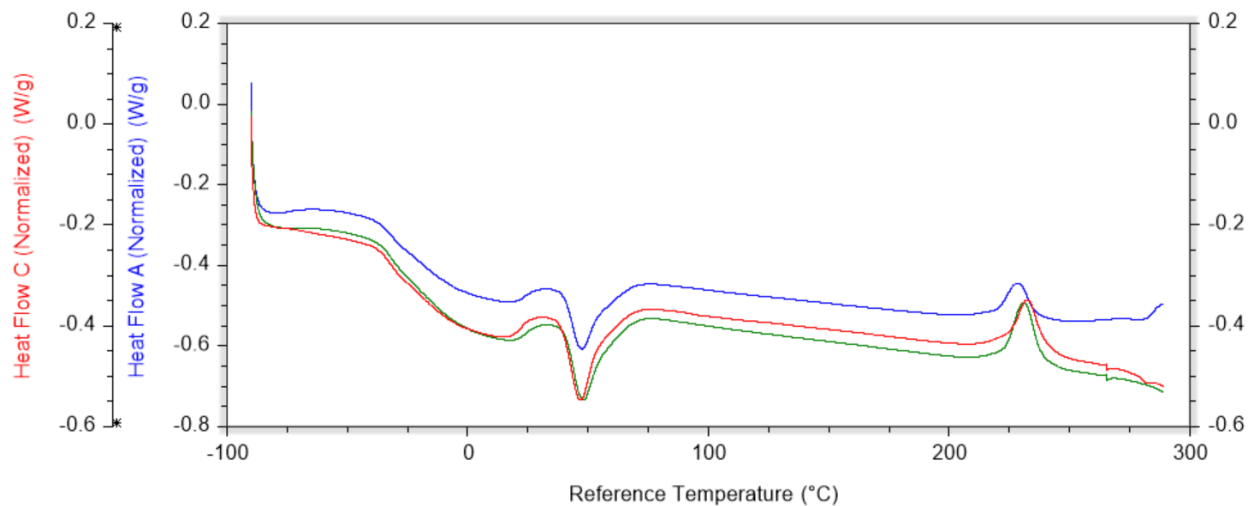


Figure S26. First heat DSC trace of EVA-2, 40% vinyl acetate. DSC trace for the first heating ramp from -90 °C to 290 °C. The three traces (A, B, and C) represent simultaneous triplicate measurements.

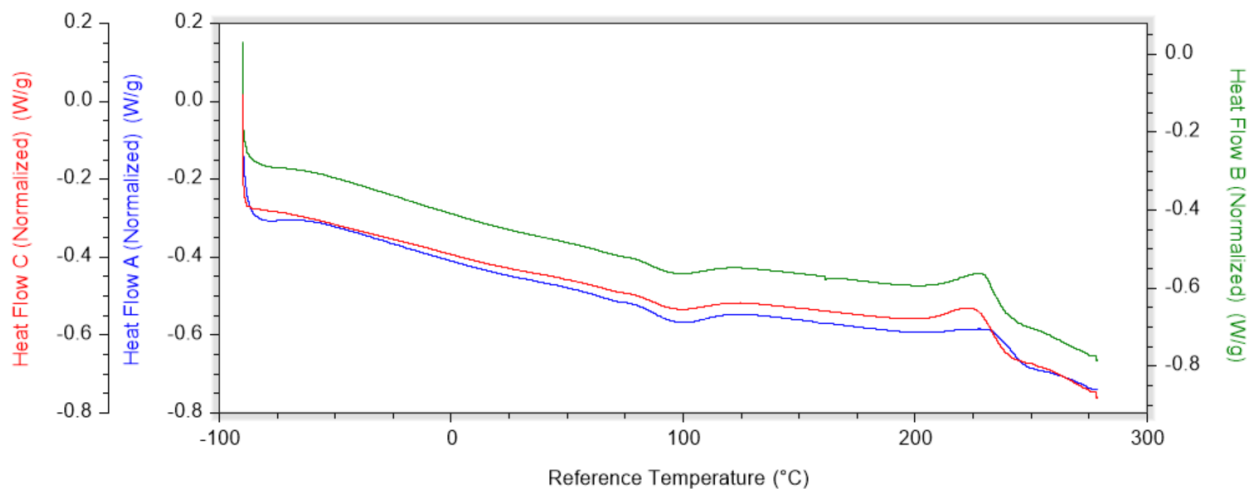


Figure S27. First heat DSC trace of PU-1. DSC trace for the first heating ramp from -90 °C to 200 °C. The three traces (A, B, and C) represent simultaneous triplicate measurements.

The following figures S28-S32 are small and wide-angle X-ray scattering (SAXS and WAXS) patterns for as-received and cryomilled polymers.

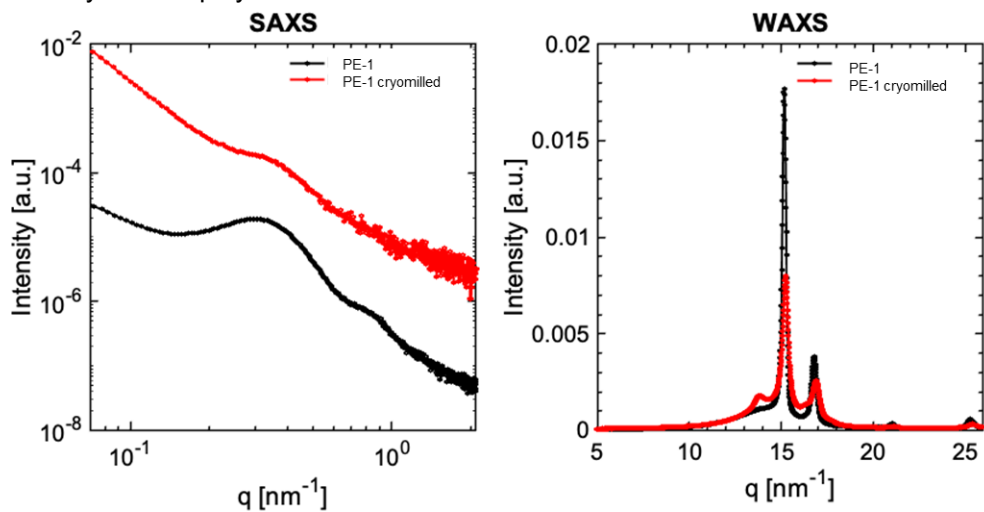


Figure S28. SAXS and WAXS patterns for as received and cryomilled PE-1.

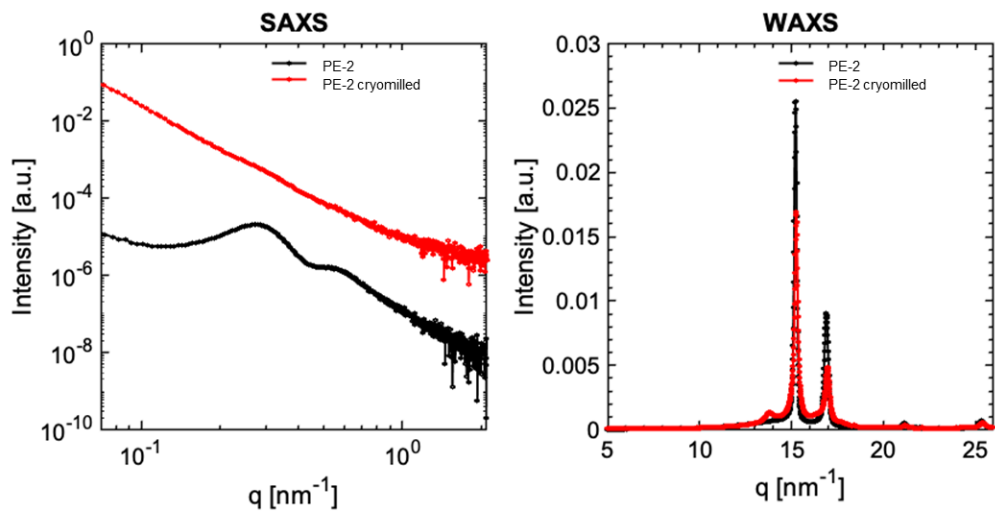


Figure S29. SAXS and WAXS patterns for as received and cryomilled PE-2.

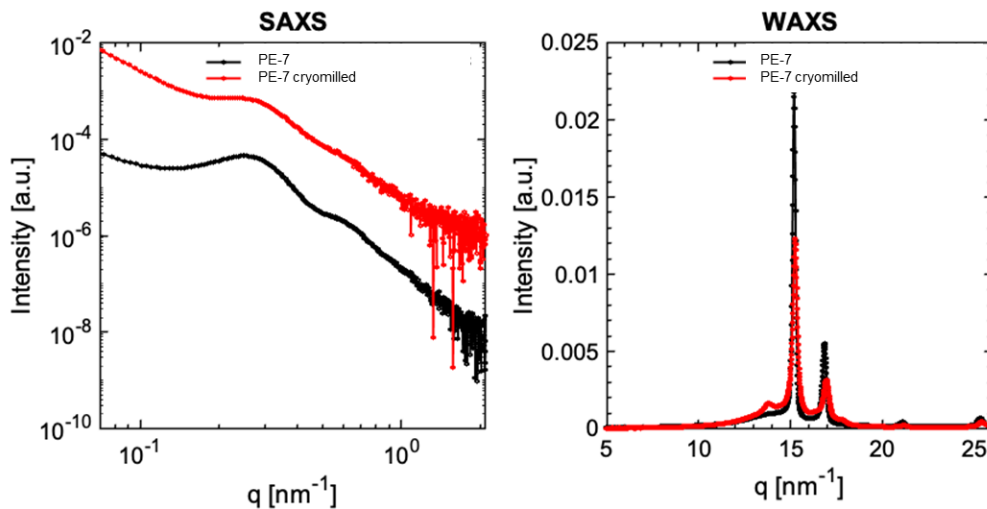


Figure S30. SAXS and WAXS patterns for as received and cryomilled PE-7.

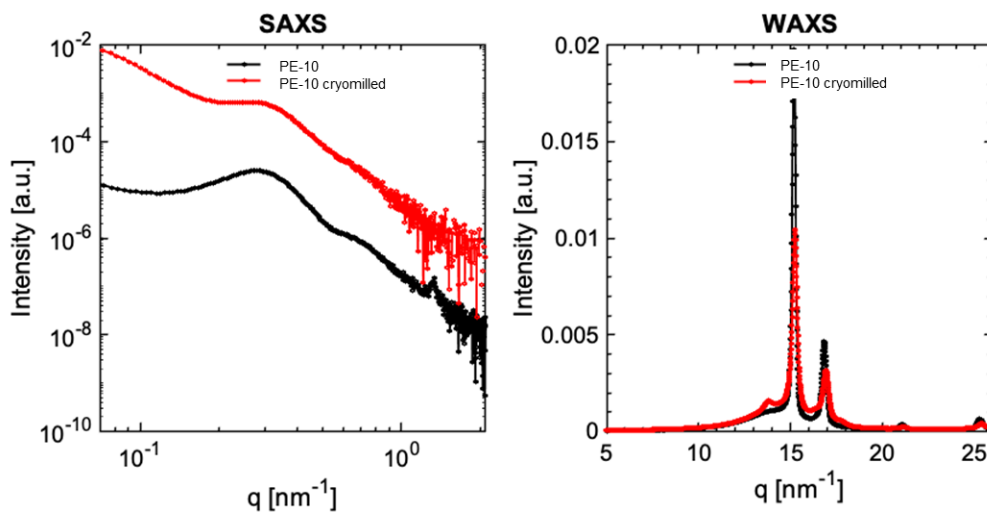


Figure S31. SAXS and WAXS patterns for PE-10.

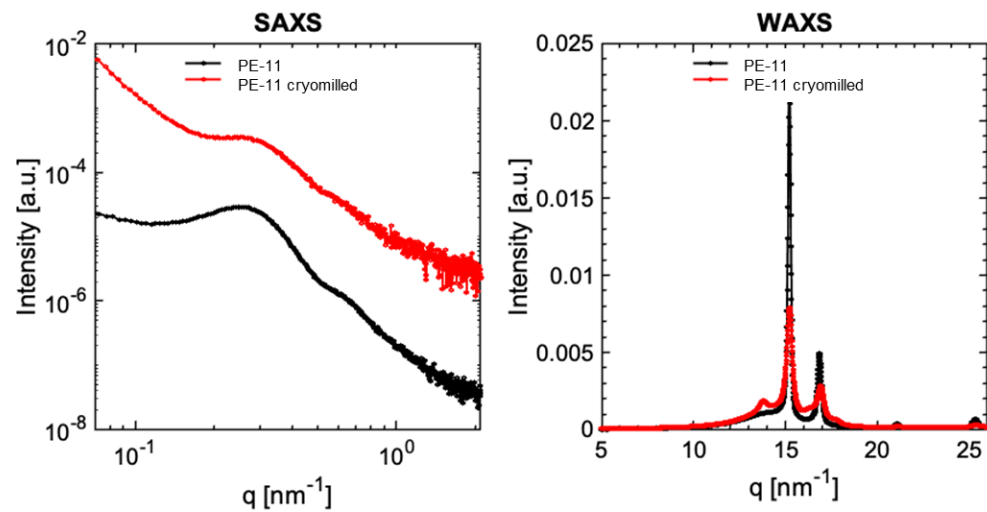


Figure S32. SAXS and WAXS patterns for as received and cryomilled PE-11.

Section V. Chemical sourcing and substrate preparation

Table S10. Chemical overview. Vendor, purity, and additional provided information for reagents.

Chemical	Vendor	Addition Information
1,1,1,3,3,3-hexafluoroisopropanol (HFIP)	Chem-Impex	≥ 99%
sodium trifluoroacetate (NaTFAc)	Sigma Aldrich	98% purity
tetrahydrofuran (THF)	Spectrum Chemical	HPLC grade; stabilized with BHT
n-hexane	EMD Millipore	LC-MS grade
ethyl acetate	Sigma Aldrich	HPLC grade
dichloromethane (DCM)	ThermoFisher Scientific	HPLC grade; stabilized with amylene
dimethyl formamide (DMF)	Sigma Aldrich	HPLC grade
1,2,4-trichlorobenzene (TCB)	Fisher Scientific	HPLC grade
lithium bromide (LiBr)	Sigma Aldrich	≥ 99%
nitric acid (HNO ₃)	EMD Millipore	67-70%, Omni Trace Ultra for trace metal analysis
fluoroboric acid (HBF ₄)	Fisher Scientific	48% aqueous
68 Component ICP-MS Standard	High-Purity Standards	3 mixes
triethanolamine	Fluka	99.5%

Text S1. Cryomilling method.

Samples were cryo-milled using a Horiba Freezer Mill 6770 (SPEX SamplePrep). A 6751C4 polycarbonate cylinder grinding vial (SPEX SamplePrep) was plugged on one end with a steel end plug. A steel impact bar was inserted into the vial. About one gram of sample was then placed into the vial, and the other end was plugged with another steel end plug. The mill's reservoir was filled with liquid nitrogen and the sample was introduced per the instruction manual. The sample was pre-cooled for 10 minutes, followed by grinding for two minutes and cooling for two minutes. The grinding and cooling steps were performed two more times for a total of seven steps in the method. The vial was allowed to thaw, and the cryo-milled sample was recovered. We were unable to cryomill polyurethane (PU) and polyketone (PK).

Section VI. Analytical methods

Text S2. GPC methods.

Weight average molar mass (M_w), number average molar mass (M_n), and polydispersity (\mathcal{D}) values were determined by gel permeation chromatography (GPC) analysis using a 1260 Infinity II LC system (Agilent), which consisted of a 1260 Iso pump module, 1260 vial sampler module, and a 1260 Multicolumn Thermostat (MCT) module. For PET, Nylon 6, Nylon 6,6, PBT, PVOH, and PMMA, the columns consisted of three PL HFIPgel 250 x 4.6 mm columns (Agilent) attached in series, along with a matching guard column. HFIP (Chem-Impex) was used as the mobile phase. It was prepared by filtering the solvent through a 0.1 μm polytetrafluoroethylene (PTFE) filter, followed by the addition of NaTFAc (Sigma Aldrich, 98% purity) to make the solution 20 mM NaTFAc. Samples were prepared in the filtered HFIP + 20 mM NaTFAc solvent at a concentration of ~ 5 mg/mL. The samples were then filtered through a 0.2 μm filter directly into a 1.5 mL GC vial. The operating conditions included a flow rate of 0.4 mL/min, a sample injection of 100 μL , and the MCT at 40 $^\circ\text{C}$. Detectors consisted of a miniDAWN TREOS Multi-Angle Light Scattering (MALS) detector (Wyatt Technology) used in combination with a Optilab T-rEX Differential Refractive Index detector (Wyatt Technology). Astra software (Wyatt Technology) was used for data analysis.

For PVC, PVAc, EVOH, PMMA, PC, PS, ABS, PU, and PLA, the columns consisted of three PLgel 10 μm Mixed-B LS 300 x 7.5 mm columns (Agilent) attached in series, along with a matching guard column. THF (Spectrum Chemical, HPLC grade, BHT stabilized) was used as the mobile phase. The THF solvent was not filtered. Samples were dissolved in THF at a concentration of ~ 5 mg/mL. PU and PLA substrates required heating at 40 $^\circ\text{C}$ for 35 minutes with gentle agitation to fully dissolve in THF. The samples were then filtered through a 0.2 μm filter directly into a 1.5 mL GC vial. All ABS samples required sequential filtrations through 1.0 μm , 0.45, and 0.2 μm PTFE filters. The operating conditions included a flow rate of 1.0 mL/min, a sample injection of 100 μL , and the MCT at 40 $^\circ\text{C}$. Detectors consisted of a miniDAWN Multi-Angle Light Scattering detector (Wyatt Technology) used in combination with an Optilab Differential Refractive Index detector (Wyatt Technology). Astra software (Wyatt Technology) was used for data analysis.

For PAN the columns consisted of three PLgel 10 μm Mixed-B LS 300 x 7.5 mm columns (Agilent) attached in series, along with a matching guard column. DMF (Sigma Aldrich, HPLC grade) amended with 10 mM LiBr (Sigma Aldrich, $\geq 99\%$) was used as the mobile phase. The DMF solvent was not filtered. Samples were dissolved in the DMF + 10 mM LiBr solvent at a concentration of ~ 5 mg/mL. The samples were then filtered through a 0.2 μm filter directly into a 1.5 mL GC vial. The operating conditions included a flow rate of 1.0 mL/min, a sample injection of 100 μL , and the MCT at 40 $^\circ\text{C}$. Detectors consisted of a miniDAWN Multi-Angle Light Scattering detector (Wyatt Technology) used in combination with an Optilab Differential Refractive Index detector (Wyatt Technology). Astra software (Wyatt Technology) was used for data analysis.

Text S3. HT-GPC methods.

High temperature gel permeation chromatography (HT-GPC) of PE, PP and EVA materials was performed using an EcoSec HLC-8321 high temperature GPC system with an autosampler and a differential refractometer (dRI) detector (Tosoh). Temperature settings were as follows, solvent stocker at 40 $^\circ\text{C}$, pump oven at 50 $^\circ\text{C}$, column oven at 160 $^\circ\text{C}$, dRI detector at 160 $^\circ\text{C}$, injector valve at 160 $^\circ\text{C}$, and autosampler at 160 $^\circ\text{C}$. TCB (Fisher Scientific, HPLC Grade) was used as the mobile phase. The TCB solvent was used as-received, and no inhibitor was added. Sample columns were set to an operating flow rate of 1.0 mL/min and the reference column was set to an operating flow rate of 0.5 mL/min. A 300 μL sample loop was used for sample injection. Polymer separation was performed using 4 TSKgel columns (Tosoh) attached in the following order, 1 x TSKgel guard column HHR (30) HT2 7.5 mm I.D. x 7.5 cm. (PN 22891), 2 x TSKgel G2000 HHR (20) HT2 7.8 mm I.D. x 30 cm columns (PN 22890), and 1 x TSKgel GMH HR-H (S) HT2 7.8 mm I.D. x 30cm column (PN 22889). A 180-minute warm-up of the instrument at 10% flow rate was performed before analysis.

Samples were prepared in 10 mL high temperature sample vials with PTFE caps (Tosoh). 6-20 mg of sample were placed on 26 μm stainless steel mesh squares (Tosoh, high temperature) and the mesh was folded around the sample. TCB was then added to the vial to reach a concentration of approximately 1.6

mg/mL. The samples were heated a 160C for 2 hours directly on the autosampler. The samples were not filtered outside of the use of the stainless-steel mesh. Polystyrene-Quick Kit-M (Tosoh, PN 21916) was used to create the calibration curve. The calibration curve was verified using polystyrene F-10 (106 kDa – PN 05210)) and F-20 (190 kDa – PN 05211) standards (Tosoh). All polystyrene standards were prepared without mesh at 1 mg/mL with no pre-heating or stirring. Run times for all standards and samples were 60 minutes.

Eco-Sec 8321 software (Tosoh) was used to evaluate calibration curves and determine molecular mass and dispersity values. All polymer RI peaks were integrated from when they first deviated from baseline to where the RI signal reached baseline signal again. Mark Houwink correction values were used to determine polyethylene molecular mass values. Mark Houwink values used for polystyrene were $K = 12.1 \times 10^{-5} \text{ dL/g}$ and $\text{Alpha} = 0.707$. Mark Houwink values used for polyethylene were $K = 40.6 \times 10^{-5} \text{ dL/g}$ and $\text{Alpha} = 0.725$. Mark Houwink values used for polypropylene were $K = 19.0 \times 10^{-5} \text{ dL/g}$ and $\text{Alpha} = 0.725$.^{1,2}

Table S11. GPC measurement conditions by polymer type. Summary of the HPLC system, solvent, column, and instrument detectors for each polymer type.

Polymer Type	HPLC System	Solvent	Columns	Detectors	Literature dn/dc; λ ; temperature
Polyethylene	EcoSec HLC-8321 (Tosoh)	TCB	one TSKgel guard HHR (30) HT2 7.5 mm I.D. x 7.5 cm., two TSKgel G2000 HHR (20) HT2 7.8 mm I.D. x 30 cm, and 1 TSKgel GMH HR-H (S) HT2 7.8 mm I.D. x 30cm	EcoSec HLC-8321 dRI (Tosoh)	N/A ^a
Polyethylene terephthalate	1260 Infinity II (Agilent), MCT at 40 °C	HFIP + 20 mM NaTFAc	three PL HFIPgel 250 x 4.6 mm and matching guard (Agilent)	miniDAWN TREOS and Optilab T-rEX (Wyatt Technology)	0.257; 632.8 nm; N/A ³
Polypropylene	EcoSec HLC-8321 (Tosoh)	TCB	one TSKgel guard HHR (30) HT2 7.5 mm I.D. x 7.5 cm., two TSKgel G2000 HHR (20) HT2 7.8 mm I.D. x 30 cm, and 1 TSKgel GMH HR-H (S) HT2 7.8 mm I.D. x 30cm	EcoSec HLC-8321 dRI (Tosoh)	N/A ^a
Polyvinyl chloride	1260 Infinity II (Agilent), MCT at 40 °C	THF	three 10 μ m Mixed-B LS 300 x 7.5 mm and matching guard (Agilent)	miniDAWN and Optilab (Wyatt Technology)	0.0961; 660 nm; 25 °C ⁴
Polystyrene	1260 Infinity II (Agilent), MCT at 40 °C	THF	three 10 μ m Mixed-B LS 300 x 7.5 mm and matching guard (Agilent)	miniDAWN and Optilab (Wyatt Technology)	0.184; 632.8 nm; 40 °C ⁵
	EcoSec HLC-8321 (Tosoh)	TCB	one TSKgel guard HHR (30) HT2 7.5 mm I.D. x 7.5 cm., two TSKgel G2000 HHR (20) HT2 7.8 mm I.D. x 30 cm, and 1 TSKgel GMH HR-H (S) HT2 7.8 mm I.D. x 30cm	EcoSec HLC-8321 dRI (Tosoh)	N/A ^a
Polyurethane	1260 Infinity II (Agilent), MCT at 40 °C	THF	three 10 μ m Mixed-B LS 300 x 7.5 mm and matching guard (Agilent)	miniDAWN and Optilab (Wyatt Technology)	N/A ^b
Acrylonitrile butadiene styrene	1260 Infinity II (Agilent), MCT at 40 °C	THF	three 10 μ m Mixed-B LS 300 x 7.5 mm and matching guard (Agilent)	miniDAWN and Optilab (Wyatt Technology)	N/A ^c
Nylon	1260 Infinity II (Agilent), MCT at 40 °C	HFIP + 20 mM NaTFAc	three PL HFIPgel 250 x 4.6 mm and matching guard (Agilent)	miniDAWN Treos and Optilab T-Rex (Wyatt Technology)	0.2375; 638.2 nm; 25 °C ³ 0.241; 638.2 nm; 25 °C ^d
Polymethyl methacrylate	1260 Infinity II (Agilent), MCT at 40 °C	THF	three 10 μ m Mixed-B LS 300 x 7.5 mm and matching guard (Agilent)	miniDAWN and Optilab (Wyatt Technology)	0.0853; 660 nm; 25 °C ⁴
Polycarbonate	1260 Infinity II (Agilent), MCT at 40 °C	THF	three 10 μ m Mixed-B LS 300 x 7.5 mm and matching guard (Agilent)	miniDAWN and Optilab, (Wyatt Technology)	0.182; 690 nm; 35 °C ⁴
Polyvinyl acetate	1260 Infinity II (Agilent), MCT at 40 °C	THF	three 10 μ m Mixed-B LS 300 x 7.5 mm and matching guard (Agilent)	miniDAWN and Optilab, (Wyatt Technology)	0.048; 610 nm; 24 °C ⁶

Ethylene vinyl acetate	EcoSec HLC-8321 (Tosoh)	TCB	one TSKgel guar HHR (30) HT2 7.5 mm I.D. x 7.5 cm., two TSKgel G2000 HHR (20) HT2 7.8 mm I.D. x 30 cm, and 1 TSKgel GMH HR-H (S) HT2 7.8 mm I.D. x 30cm	EcoSec HLC-8321 dRI (Tosoh)	N/A ^a
Polyvinyl alcohol	1260 Infinity II (Agilent), MCT at 40 °C	HFIP + 20 mM NaTFAc	three PL HFIPgel 250 x 4.6 mm and matching guard (Agilent)	miniDAWN TREOS and Optilab T-rEX (Wyatt Technology)	N/A ^c
Ethylene vinyl alcohol	1260 Infinity II (Agilent), MCT at 40 °C	THF	three 10 µm Mixed-B LS 300 x 7.5 mm and matching guard (Agilent)	miniDAWN and Optilab (Wyatt Technology)	N/A ^c
Polylactic acid	1260 Infinity II (Agilent), MCT at 40 °C	THF	three 10 µm Mixed-B LS 300 x 7.5 mm and matching guard (Agilent)	miniDAWN and Optilab (Wyatt Technology)	N/A ^b
Polyacrylonitrile	1260 Infinity II (Agilent), MCT at 50 °C	DMF + 10 mM LiBr	three 10 µm Mixed-B LS 300 x 7.5 mm and matching guard (Agilent)	miniDAWN and Optilab (Wyatt Technology)	0.084; 690 nm, 60 °C ⁷
Polybutylene terephthalate	1260 Infinity II (Agilent), MCT at 40 °C	HFIP + 20 mM NaTFAc	three PL HFIPgel 250 x 4.6 mm and matching guard (Agilent)	miniDawn Treos and Optilab T-Rex (Wyatt Technology)	N/A ^b
Polyketone	1260 Infinity II (Agilent), MCT at 40 °C	HFIP + 20 mM NaTFAc	three PL HFIPgel 250 x 4.6 mm and matching guard (Agilent)	miniDAWN TREOS and Optilab T-rEX (Wyatt Technology)	N/A ^b
Polyhydroxy butyrate	1260 Infinity II (Agilent), MCT at 40 °C	HFIP + 20 mM NaTFAc	three PL HFIPgel 250 x 4.6 mm and matching guard (Agilent)	miniDAWN TREOS and Optilab T-rEX (Wyatt Technology)	N/A ^b
Styrene acrylonitrile	1260 Infinity II (Agilent), MCT at 40 °C	THF	three 10 µm Mixed-B LS 300 x 7.5 mm and matching guard (Agilent)	miniDAWN and Optilab (Wyatt Technology)	N/A ^c

^aLiterature dn/dc was not used for polymers measured using column calibration.

^bNo appropriate literature value was found.

^cNo appropriate literature value was found, and dn/dc is dependent on copolymer ratio.

^dFor nylon-6

Text S4. Differential Scanning Calorimetry (DSC) Methods.

Differential scanning calorimetry (DSC) was used to characterize both the pristine and cryomilled polymers. DSC measurements were simultaneously performed in triplicate on a Discovery X3 Differential Scanning Calorimeter (TA Instruments) using 7-10 mg of sample in hermetically sealed aluminum pans (DSC Consumables). Each DSC run consisted of two heating and cooling cycles at a rate of 10 °Cmin⁻¹ with 5-minute isothermal holds between each heating and cooling ramp. The minimum and maximum temperature of the heating and cooling cycles was dependent on each type of polymer (**Table S8**). The glass transition temperature (T_g), melting temperature (T_m), enthalpy of melting (ΔH_m), crystallization temperature (T_c), temperature of cold crystallization (T_{cc}), and enthalpy of cold crystallization (ΔH_c) for each polymer determined when applicable with TRIOS software (Universal Analysis). **Equation S1** was used to calculate percent crystallinity, where ΔH_m° is the reference enthalpy of melting (**Table S12**).

Equation S1. Percent crystallinity equation.

$$\% \text{ Crystallinity} = \left(\frac{\Delta H_m - \Delta H_c}{\Delta H_m^\circ} \right) \cdot 100\%$$

Table S12. DSC temperature bounds and enthalpy of melting by polymer class. Minimum and maximum temperatures used for each polymer type for DSC analysis.

Polymer Type	Minimum Ramp Temperature (°C)	Maximum Ramp Temperature (°C)	ΔH_m° (Jg ⁻¹)
PVC	0.0	220.0	
PVAc	-90.0	250.0	138 ⁸
PVOH	0.0	250.0	161 ⁹
EVA	-90.0	290.0	
EVOH	-90.0	210.0	199-219 ^{10, a}
PMMA	-90.0	175.0	
Nylon-6	0.0	290.0	230 ⁹
Nylon-6,6	0.0	290.0	226 ⁹
PS	-90.0	270.0	
PE	-90.0	160.0	293 ⁹
PC	-90.0	280.0	
PP	-90.0	265.0	207 ⁹
PET	0.0	300.0	140 ⁹
PAN	-90.0	315.0	
PBT	0.0	300.0	146 ⁹
ABS	-90.0	175.0	
PU	-90.0	200.0	
Polyketone	0.0	250.0	
PLA	-90.0	180.0	
PHB	-90.0	210.0	146 ¹¹
SAN	-90.0	175.0	

^aEnthalpy of melting is depending on copolymer composition and was calculated as described by Luzi et al.¹⁰

Equation S2. Standard deviation equations. Statistical analysis was conducted using an independent two-sample t-test using a pooled standard deviation to determine the t-value. The t-value was calculated using the averages between values (X_1 and X_2) with degrees of freedom $n = N-1$. The pooled standard deviation uses the standard deviation for each set (S_{x1} and S_{x2})

$$t = \frac{X_1 - X_2}{s_p \sqrt{\frac{2}{n}}}$$

$$s_p = \sqrt{\frac{S_{x1}^2 + S_{x2}^2}{2}}$$

Text S5. TGA-FTIR EGA Analysis.

For each measured substrate, 7-10 mg of sample was loaded into a pre-tared 110 μL platinum TGA pan. The pan was then placed into a Discovery SDT 650 instrument (TA Instruments) connected to a FTIR Spectrum 3 spectrometer (Perkin Elmer), equipped with a TL 8000 Balanced Flow FT-IR EGA system (Perkin Elmer). A TGA-IR Interface TL 8000e (PerkinElmer) was used to set the temperature of the adapter, cell, and TL-TGA of the EGA System to a temperature of 270 $^{\circ}\text{C}$ and a flow rate 70 mLmin^{-1} . A background spectrum was performed on the Spectrum 3 before each sample was run with a resolution of 4 cm^{-1} and an accumulation set to 64 scans. The sample pan was then heated under nitrogen (100 mLmin^{-1}) from ambient temperatures to 700 $^{\circ}\text{C}$ at a ramp rate of 50 $^{\circ}\text{Cmin}^{-1}$. A simultaneous experiment was conducted on the Spectrum 3 to analyze the evolved gas from the Discovery SDT 650 using a wavenumber range from 650-4000 cm^{-1} , a resolution of 4 cm^{-1} , and an accumulation set to 2 scans. The pan was cleaned after each run by running an isotherm at 700 $^{\circ}\text{C}$ for 10 minutes. All TGA curves were analyzed using TRIOS software (TA Instruments) while all FTIR spectra were analyzed using Spectrum IR software (Perkin Elmer).

Text S6. SAXS and WAXS Methods.

Sample Preparation for SAXS and WAXS measurement: Powder samples were placed between two thin Kapton[®] films using washers. Pellet samples were attached to Kapton[®] tape (thickness 0.063 mm), while film samples were directly placed on the sample holder for transmission SAXS and WAXS measurements. Backgrounds from Kapton[®] films, tape, and air were measured for each sample to perform background subtraction during data correction.

Small-angle X-ray scattering (SAXS): The small-angle X-ray scattering (SAXS) experiment was performed at 1-5 beamline of Stanford Synchrotron Radiation Lightsource, SLAC National Laboratory in Menlo Park, USA. The beamline 1-5 was equipped with ion chambers both upstream and downstream to ensure data normalization. A photon counting area detector, Pilatus 1M (1120 \times 967 pixels, 172 \times 172 μm^2 pixel size; Dectris AG, Switzerland), was utilized for SAXS measurement. The X-ray beam was micro-focused, with a spot size of approximately 500 \times 500 μm^2 and had an energy of 15 keV. The sample-to-detector-distance (SDD) was \sim 2.8 m. The SDD was calibrated using the silver behenate standard sample. This setup offered a resolvable q-range of 0.07-2.1 nm^{-1} . Powder samples and 2 layers of Kapton[®] thin film were measured for a total time of 4.5 minutes (3 spots, 3 frames of 30 seconds for each spot). Pellet samples and Kapton[®] tape were measured total time of 2 minutes (1 spot with 4 frames for 30 seconds each). Thin film samples and air as background were measured at 3 spots, with 3 frames of 30 seconds for each spot, total time of 4.5 minutes, in transmission mode.

Wide-angle X-ray scattering (WAXS): The wide-angle X-ray scattering (WAXS) measurement was carried out at 11-3 beamline of the Stanford Synchrotron Radiation Lightsource, SLAC National Laboratory in Menlo Park, USA. Beamline 11-3 was equipped with a beamstop, which contained an inbuilt photodiode for measuring the transmitted intensity and an MX225 fiber-optic based CCD area detector (3072 \times 3072 pixels, 73 \times 73 μm^2 pixel size; Rayonix, L.L.C. USA). The measurement employed an X-ray beam with a spot size of \sim 150 \times 150 μm^2 , an energy of 12.7 keV, and a sample-to-detector-distance (SDD) of \sim 350 mm. The SDD was calibrated using the standard Lanthanum hexaboride (LaB6). Powder samples and 2 layers of Kapton[®] thin film as background were measured at 1 spot, with 6 frames of 10 seconds. Pellet samples and Kapton[®] tape (thickness 0.063 mm) were measured at 1 spot with 15 frames for 2 seconds each. The

thin film sample and air as background were measured at 1 spot in transmission mode, with 6 frames of 10 seconds for each spot.

SAXS and WAXS data reduction and correction: To obtain a 1D radial profile from SAXS and WAXS data, all 2D frames measured for each sample were averaged and the data was reduced using the Nika package for Igor Pro 8.04.¹² Additionally, data correction was performed using MATLAB (R2021a) scripts.

For SAXS data, the extracted 1D profile was normalized to the incident flux and transmitted flux using up- and downstream ion chambers.¹³ Subsequently, the background was subtracted from the sample data.

As for the WAXS data, the extracted 1D profile of samples and their corresponding background were normalized to the Kapton® peak observed at approximately 4 nm⁻¹. After this normalization, the background was subtracted from the sample data. Finally, the 1D subtracted WAXS profiles were further normalized to the sum of scattering intensity between $q=5-25$ nm⁻¹, allowing for a comparison between the cryomilled sample and the as-received samples.

Text S7. CHNS Method

The polymer samples were analyzed for carbon, hydrogen, nitrogen, and sulfur using a CHN 628 series with a Sulfur Add-on Module (S628) (LECO Corporation). The samples were measured for CHN and S using separate methods.¹⁻³ For CH and N, 80-100 mg of samples were measured and wrapped into a tin cup. The CHN method combustion temperature was 950 °C and the afterburner temperature was 850 °C. The burn profile was a high furnace flow for 40 seconds, then a medium furnace flow for 30 seconds, and finally a high furnace flow for 30 seconds. The ballast had an equilibration time of 30 seconds with a 300 second not filled timeout. The aliquot loop had a fill pressure drop of 200 mmHg with an equilibration time of 8 seconds. The CHN method was calibrated using EDTA (LECO Corporation). **Table S9** contains the elemental parameters for CH and N. For S analysis, 80-100 mg of sample were measured and loaded into ceramic boats. The S method parameters were as follows: furnace temperature of 1350 °C, manual load baseline delay time of 3 seconds, minimum analysis time of 90 seconds, comparator level of 0.30%, endline time of 1 second, conversion factor of 1.00, 5 significant digits, IR analysis stabilize comparator of 2.00, IR baseline time of 1 second, and an auto detect data missed time of 5 seconds. Ceramic boats containing sample were manually loaded into the furnace.

Table S13. Elemental Parameters for CHNS Analysis.

	Carbon	Hydrogen	Nitrogen
Baseline Delay (s)	0	0	10
Min Analysis Time (s)	20	40	40
Comparator Level	100	100	100
Endline Time (s)	1	1	2
Conversion Factor	1	1	1
Significant Digits	5	5	5
IR Baseline Time (s)	-	-	1
TC Baseline Time (s)	-	-	10

Text S8. Conditions for the ultraWAVE digester.

200-250 mg of cryomilled (when possible) sample was digested in either 4 mL high purity nitric acid, or 4 mL + 1 mL fluoroboric acid + 1 mL Milli-Q water. These were run using the following conditions in **Table S14**.

Table S14. Ramping conditions for the ultraWAVE digester.

Step	Time	T1 °C	T2 °C	Pressure 1 (bar)	Energy (watts)
1	00:10:00	110	60	90	800
2	00:10:00	180	60	100	1000
3	00:10:00	250	60	130	1500
4	00:15:00	250	60	130	1500

Text S9. Gas Chromatography Mass Spectrometry Flame Ionization Detection (GC-MS/FID) methods.

Samples were analyzed using an 8890 GC (Agilent) coupled to a 5877 MSD (Agilent) using a ZB-5 Inferno column (Phenomenex) with a maximum temperature of 430 °C. This instrument has a capillary flow technology (CFT) plate that splits the sample flow onto two detectors, a mass spectrometry detector (MSD) and a flame ionization detector (FID) at a 1:4 split ratio. The inert columns used from the CFT plate to each detector was rated for a maximum temperature of 430 °C. 1 µL of each sample were injected into the inlet port at 280 °C in splitless mode. The oven ramp temperature started at 40 °C, was held for 2 minutes and then ramped at 9°Cmin⁻¹ to 340 °C. The transfer line temperature to the MSD was held at 350 °C. The MSD was in electron ionization (EI) mode at 70 eV, with the MS source temperature at 230 °C and the quadrupole temperature at 150 °C. The instrument was extraction source tuned (etuned) prior to analysis. The FID detector temperature was held at 315° C.

References

1. Agilent, *Technical overview: Repeatability in high temperature polyethylene analysis using Agilent PLgel MIXED-B*, Agilent.
2. T. G. Scholte, N. L. J. Meijerink, H. M. Schoffeleers and A. M. G. Brands, *Journal of Applied Polymer Science*, 1984, **29**, 3763-3782.
3. S. Mori, Barth, H.G., *Size Exclusion Chromatography*, 1999.
4. A. M. Striegel, *Chromatographia*, 2017, **80**, 989-996.
5. L. Jeng, S. T. Balke, T. H. Mourey, L. Wheeler and P. Romeo, *Journal of Applied Polymer Science*, 1993, **49**, 1359-1374.
6. A. E. Hamielec, A. C. Ouano and L. L. Nebenzahl, *Journal of Liquid Chromatography*, 1978, **1**, 527-554.
7. J. D. Moskowitz, *Dissertations*, 2015, **173**.
8. O. W. Guirguis and M. T. H. Moselhey, *Natural Science*, 2012, **04**, 57-67.
9. R. L. Blaine, TA Instruments, Polymer Heats of Fusion, New Castle, DE www.tainstruments.com/pdf/literature/TN048.pdf.
10. F. Luzi, L. Torre and D. Puglia, *Molecules*, 2020, **25**.
11. P. J. Barham, A. Keller, E. L. Otun and P. A. Holmes, *Journal of Materials Science*, 1984, **19**, 2781-2794.
12. J. Ilavsky, *Journal of Applied Crystallography*, 2012, **45**, 324-328.
13. B. R. Pauw, *Journal of Physics: Condensed Matter*, 2013, **25**, 383201.